

https://dspace.org/

Characterization of 1-ACBP B-ACBP and PBR in oesophageal cancer

McCabe, Michelle Lynn

2006-10-27T07:44:47Z
http://hdl.handle.net/10539/1484

Downloaded from a DSpace repository. https://dspace.org/

3.1.1 Normal Oesophagus

The normal oesophagus consists of seven layers; lamina propria, muscularis mucosa, submucosa, circular (skeletal) muscle layer, connective tissue, longitudinal (skeletal) muscle layer, and the adventitia. The lumen of the normal oesophagus is surrounded by the mucosa, submucosa, muscularis propria, and external connective tissue. The mucosa is composed of stratified, non-keratinising squamous epithelium, the lamina propria, superficial submucosal glands, and muscularis mucosa, which produce local movements and folding of the mucosa (view figure 13). The submucosa consists of deep submucosal glands, which aid lubrication, and the muscularis contains inner circular and outer longitudinal layers of smooth muscle, which is the basis of peristaltic contraction (Wheater et.al, 1979). The submucosa and muscularis propria contain lymphatic channels, and this lymphatic drainage accounts for the spread of primary oesophageal carcinomas (Troncoso and Riddell, 1985). The adventitia is the outer connective tissue that conducts the major vessels and nerves (Wheater et.al., 1979).

3.1.2 Cancer of the Oesophagus

Tumours can be well, moderately, or poorly differentiated and different degrees of differentiation can be seen within the same tumour. Regardless of the degree of differentiation of the tumour, extensive infiltration of the oesophageal wall and lymphatic invasion are frequently present.

Benign tumours are well differentiated and disclose the same general cytoplasmic and nuclear ultrastructure found in normal cells, while a malignant tumour is a progressive

growth of poorly differentiated tissue that shows distorted, disorganized and misshapen nuclei and cytoplasmic organelles. Malignant tumours tend to invade surrounding normal tissues and spreads to other parts of the body by way of lymphatic channels or blood vessels View figures 14-20.

Squamous carcinoma: CIS of squamous oesophageal epithelium is characterized by the change in the thickness of the mucosa being replaced by epithelial cells that fail to mature as the surface is approached, and cytologically by pleomorphic nuclei that are usually hyperchromatic and have lost their usual orientation (Troncoso and Riddell, 1985).

There are 4 different types of squamous carcinoma namely: Superficial carcinoma, Verrucuos carcinoma, Squamous cell carcinoma with a spindle cell component, and Small-cell variant (Troncoso and Riddell, 1985).

(1) *Superficial carcinoma* is and early form of invasive squamous carcinoma with limited involvement of the mucosa and submucosa, and lesions vary from 1-5cm in size. These carcinomas are rare, but carry a much better prognosis than conventional squamous carcinoma, view figure 15.

(2) *Verrucuous carcinoma* is an exophytic papillary growth that grows slowly and if it does invade, does so locally with a low metastasising potential It is also a rare squamous carcinoma type and deep biopsies are required to determine if it is invasive or not (Minielly, et al., 1967).

(3) *Squamous cell carcinoma* with a spindle cell component contains a polyploid lesion and contains an exuberant spindle cell component and can be benign or

malignant, these too are rare. These neoplasms can reach a considerable size, and tumours up to 15 cm in diameter (Moore et al., 1963).

(4) *Small-cell carcinoma* is a rare tumour as well, and three morphological variants are included in this group. These include a small-cell variant of squamous carcinoma, an oat-cell-like tumour (APUDoma), and a combination of both (Reid et al., 1980; Rosen et. al, 1975).

Adenocarcinoma: Adenocarcinoma can arise from the oesophageal mucosal glands, submucosal glands, heterotopic gastric mucosa or from the columnar-lined Barret's oesophagus (BE), view figure 21. The gross appearances of adenocarcinomas are similar to those seen in squamous carcinoma, extensive infiltration of the wall and lymphatics spread are common at the time of diagnosis (Troncoso and Riddell, 1985). Low-grade dysplasia of BE includes gland architecture that is not abnormal, but the epithelial cells have enlarged hyperchromatic nuclei that occupy the lower half of the cells, and the cellular abnormalities extend to the surface of the mucosa. High-grade dysplasia involves glands that are irregular and tightly packed, enlarged and irregular cell nuclei that exhibit abnormal chromatin patterns. Early invasive adenocarcinoma is recognized by the presence of angulated glands, irregular groups of cells or single cells in the lamina propria, and a desmoplastic stromal response (Antonioli & Wang, 1997).

H&E staining of normal and diseased oesophageal tissue sections

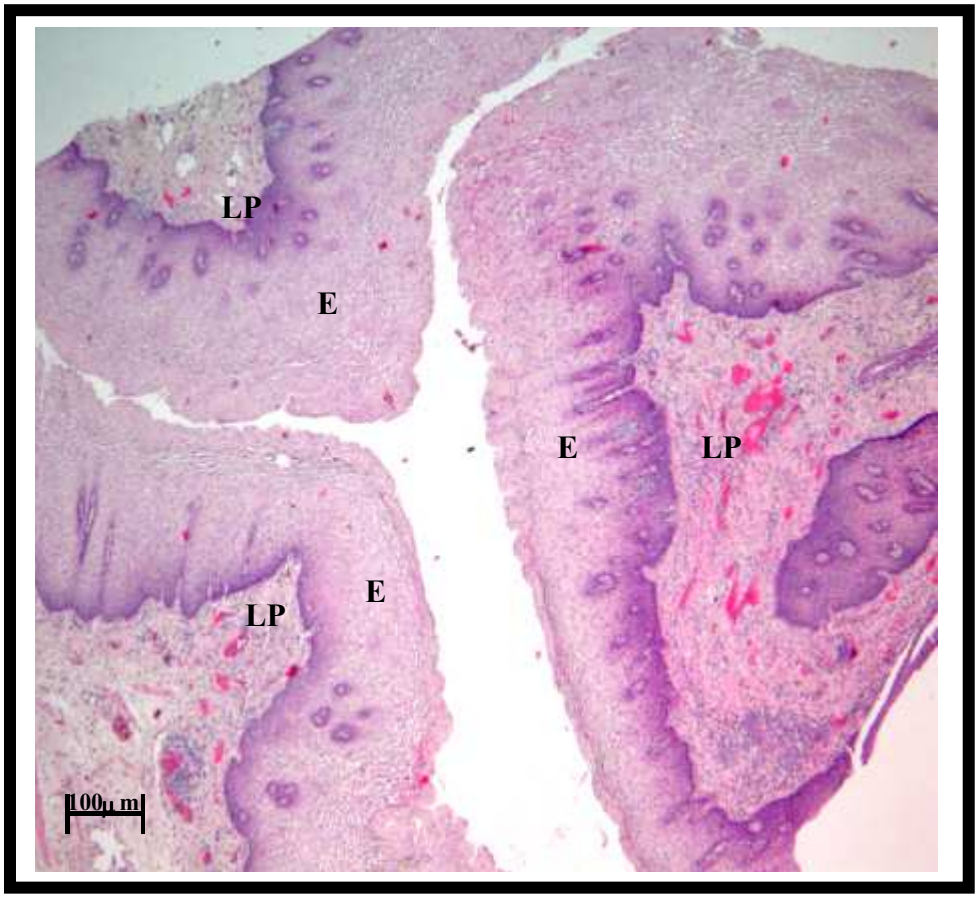

Figure 14: H&E of a normal oesophageal tissue section

This micrograph is illustrates a normal oesophageal tissue section, where the first two layers of the mucosa is shown, consisting of an inner lining of nonkeratinized stratified epithelium (**E**) and a layer of fine connective tissue, the lamina propria (**LP**). The micrograph was captured with a Zeiss camera attached to a light microscope. Magnification X100. Stain: Hematoxylin and Eosin staining.

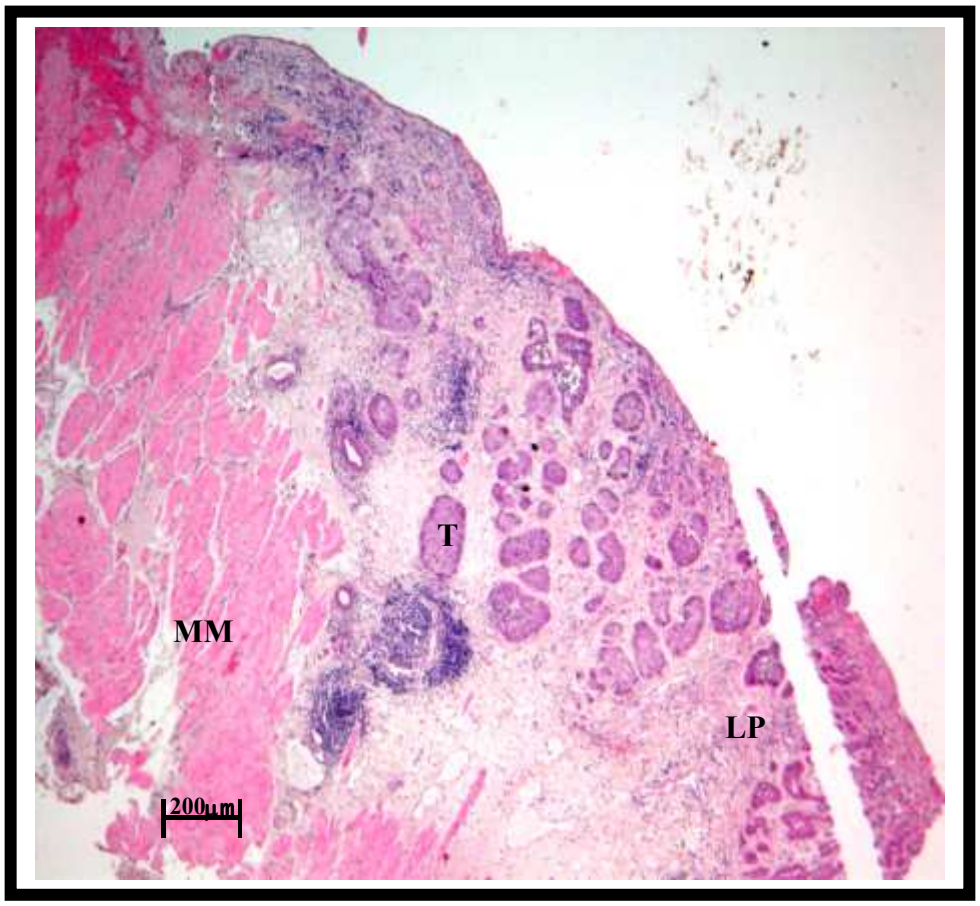

Figure 15: High grade invasive squamous cell carcinoma

This micrograph shows the oesophageal biopsy of a patient with a high grade oesophageal squamous carcinoma. The presence of an invasive moderately differentiated keratinizing squamous cell carcinoma was diagnosed. As seen the tumour (**T**) shows infiltration into fibres of the muscularis mucosa (**MM**) from the lamina propria (**LP**). Magnification X100. Stain: Hematoxylin and Eosin.

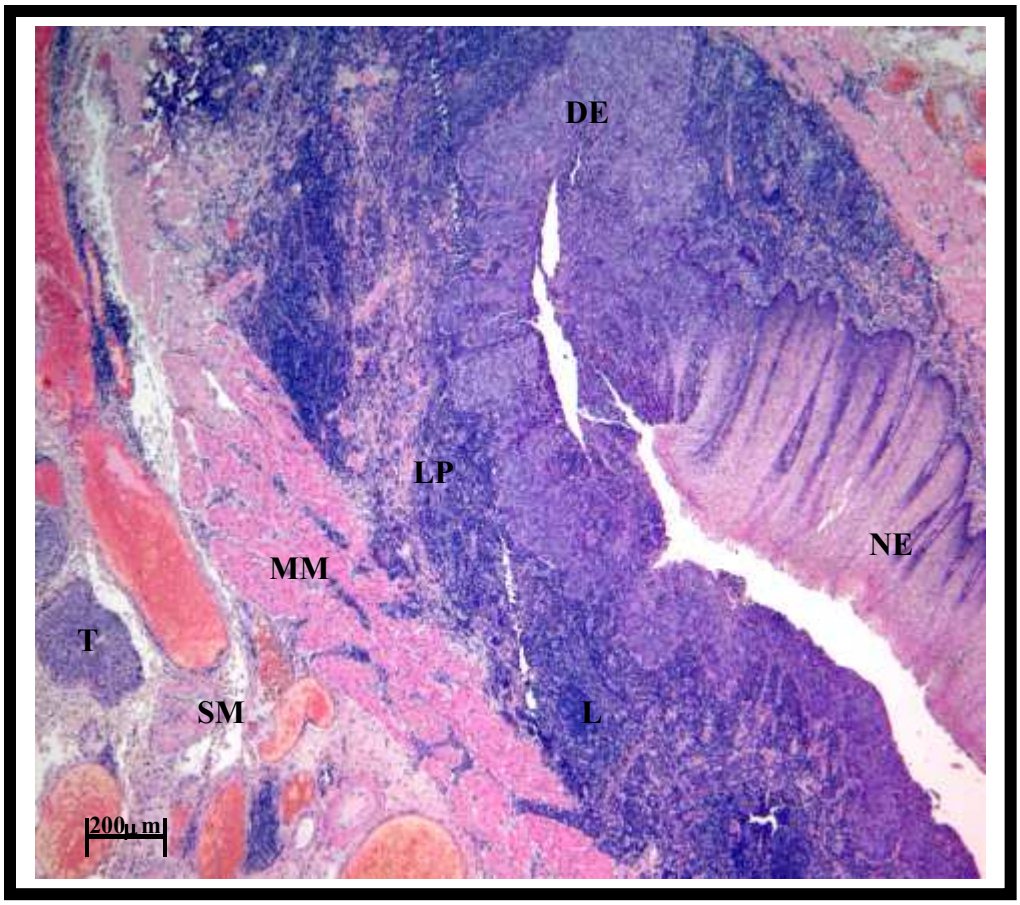

Figure 16: H&E of a high grade squamous cell carcinoma

This micrograph shows the biopsy of a patient with high grade oesophageal squamous carcinoma. The mucosa here shows areas of full thickness epithelial dysplasia, arising from an invasive moderately differentiated, keratinizing squamous cell carcinoma. Lymphocytes (**L**) are highly active in the lamina propria. It infiltrates into the underlying submucosa (**SM**) and through the wall, and is present at the adventitial margin (but not shown in this micrograph). Magnification X100. Stain: Hematoxylin and Eosin.

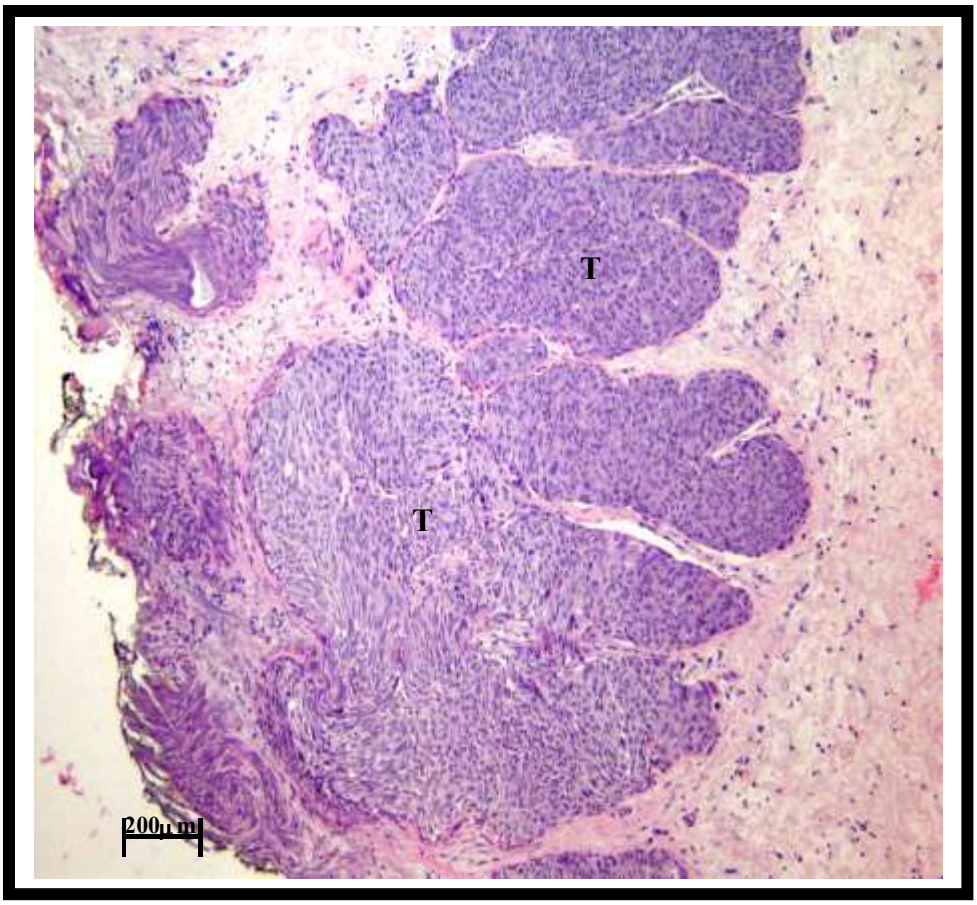

Figure 17: H&E of a tumour in a high-grade squamous cell carcinoma

Here is a tumour in a high grade, invasive, and moderately differentiated keratinizing squamous cell carcinoma. The tumour shows a swirling growth pattern which invades the rest of the tissue. Hematoxylin and Eosin staining (X100).

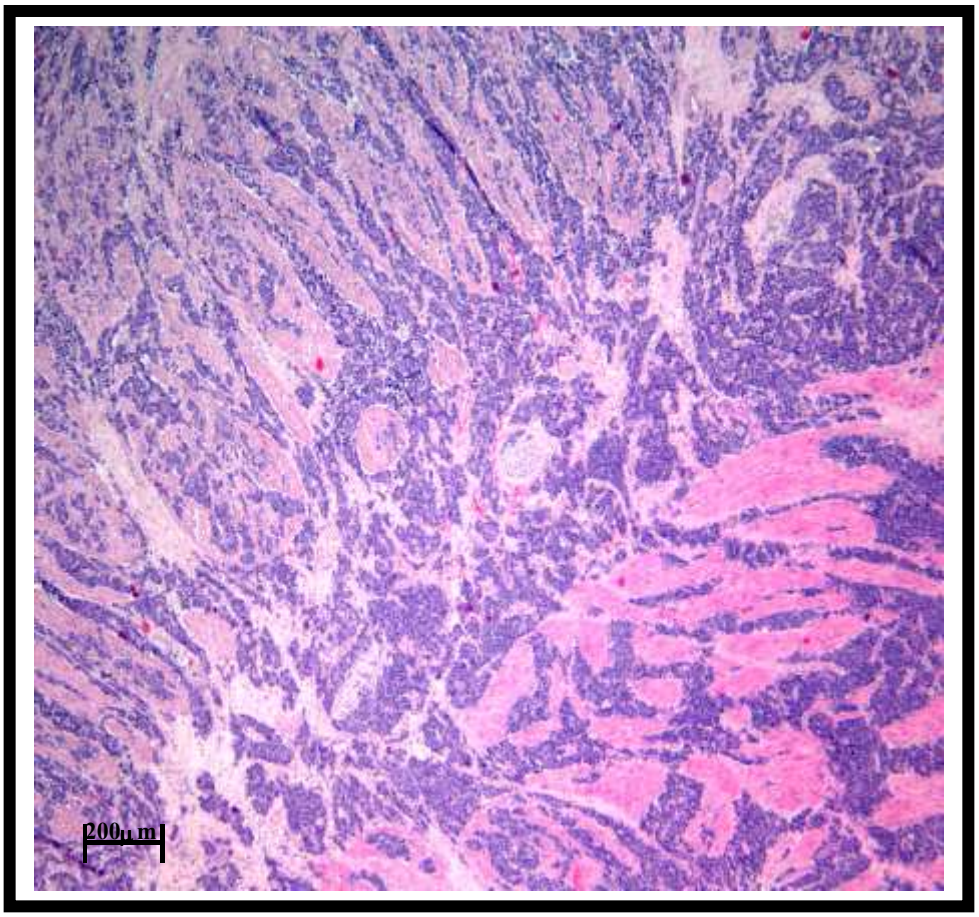

Figure 18: H&E of a high grade in-situ squamous cell carcinoma

This micrograph illustrates a high grade, poorly differentiated focally keratinizing squamous cell carcinoma, with an in-situ squamous cell carcinomatous component. There is a transmural involvement of the oesophageal wall, with tumour extending into the adventitial margin. Magnification X100. Stain: Hematoxylin and Eosin.

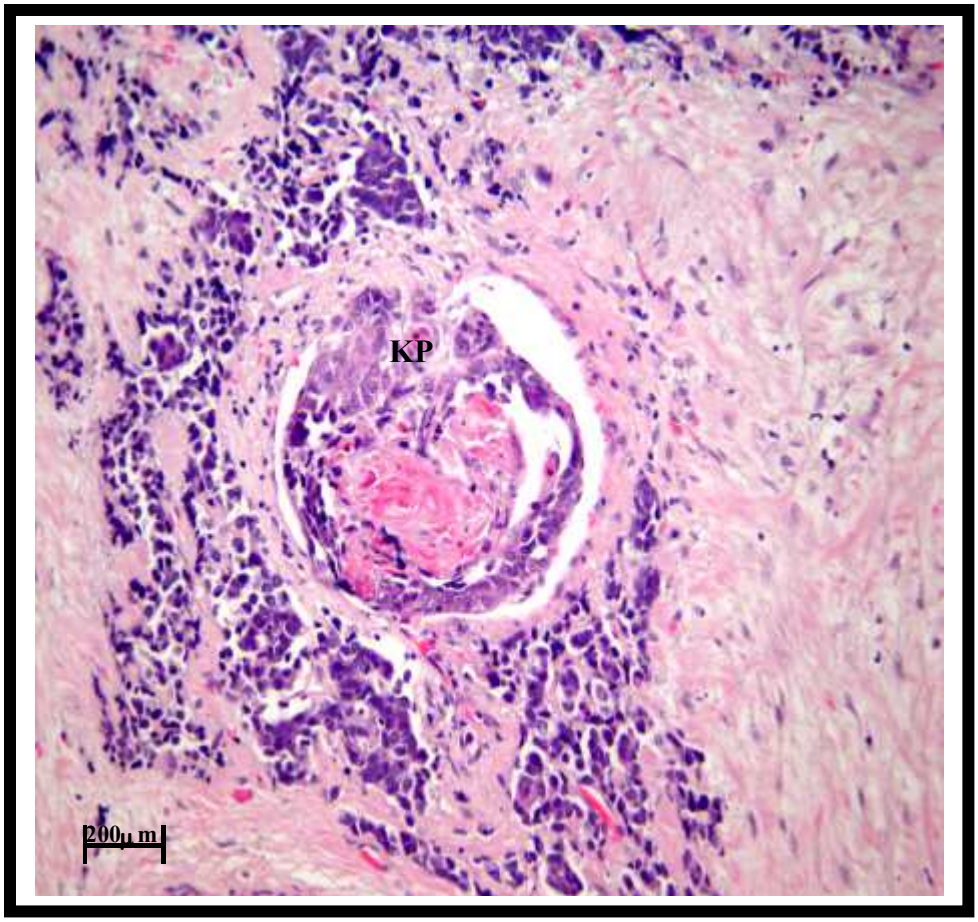

Figure 19: H&E of a Keratin Pearl in a high grade in-situ squamous cell carcinoma

Aberrant keratinization is a feature of squamous cell carcinoma and results in the formation of intraepithelial keratin pearls (**KP**). Magnification X200. Stain: Hematoxylin and Eosin.

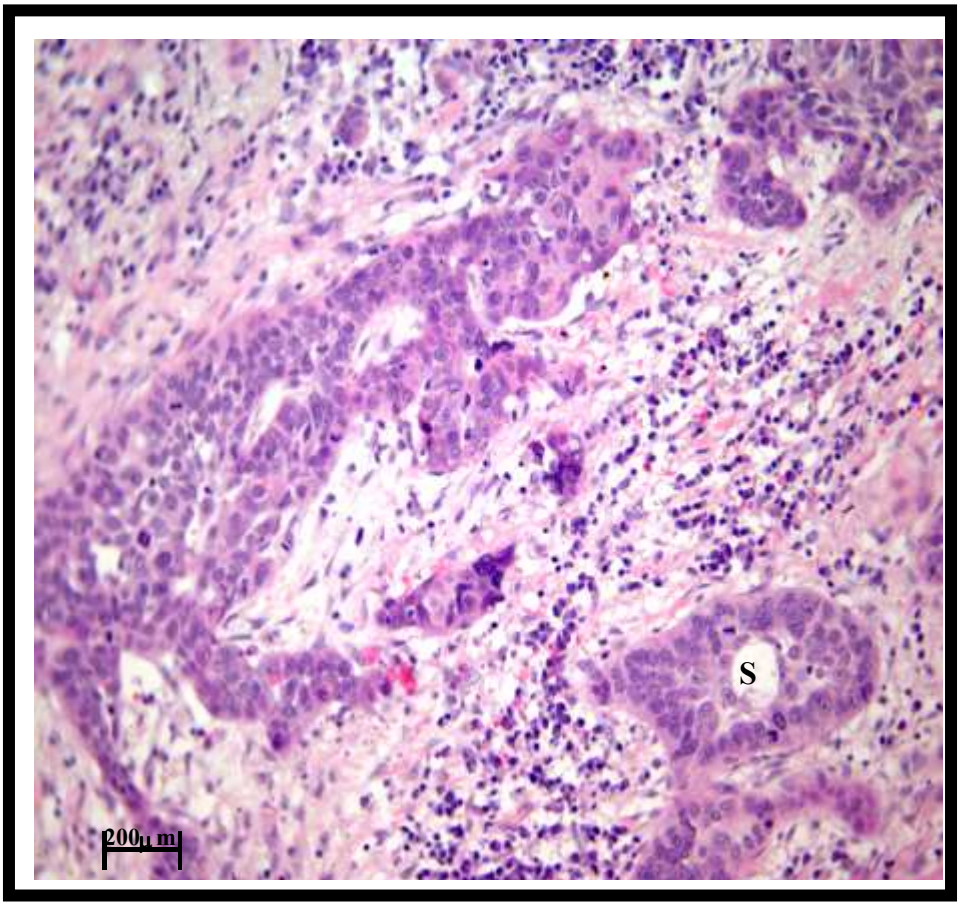

Figure 20: Signal cell in a high grade squamous cell carcinoma

A signal cell is shown here in a high grade infiltrating moderately differentiated squamous cell carcinoma. Magnification X200. Stain: Hematoxylin and Eosin.

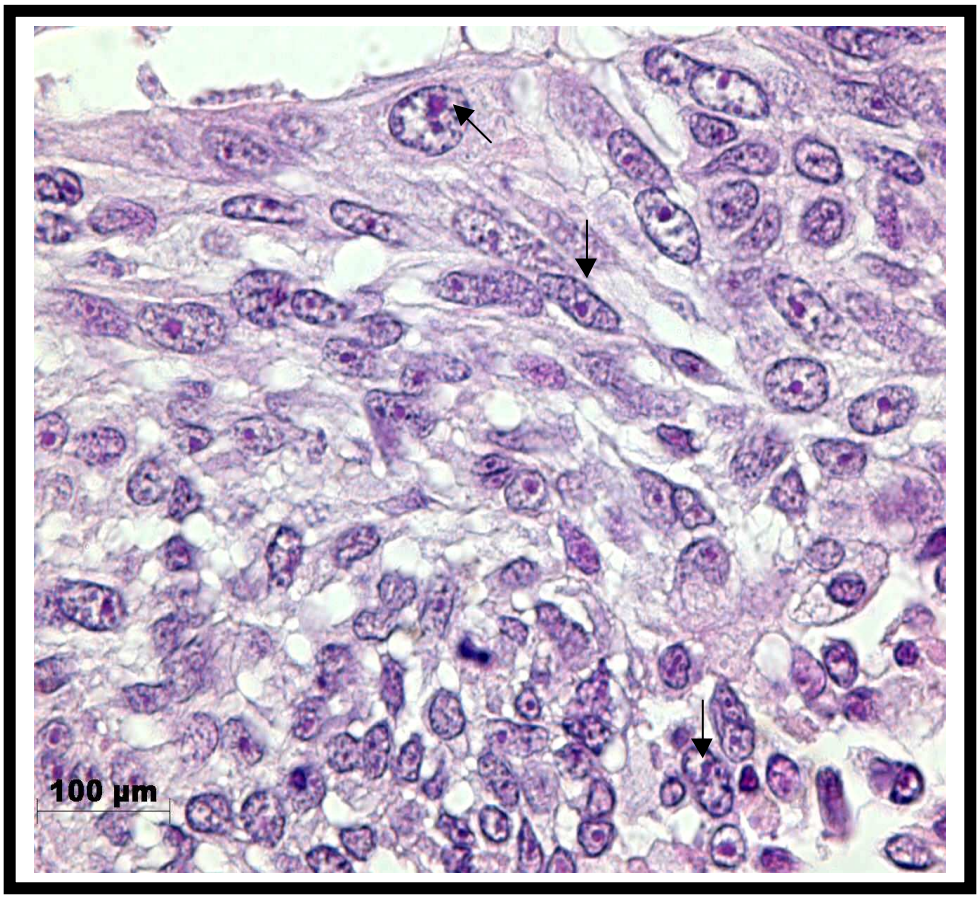

Figure 21: Epithelium of a high-grade squamous cell carcinoma

This micrograph illustrates a squamous epithelial layer of a well differentiated squamous cell carcinoma. A high number of mitotic bodies are present with irregular cell structure and hyperchromatic nuclei occurring. Magnification X1000. Stain: Hematoxylin and Eosin.

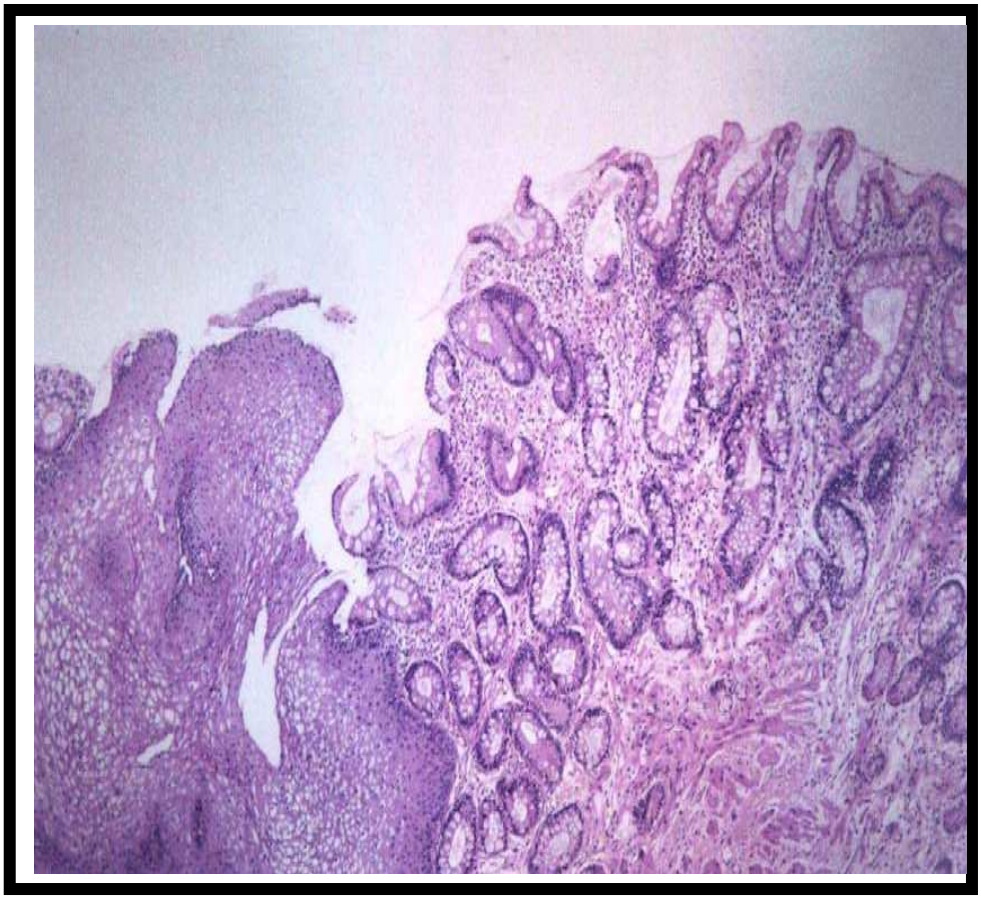

Figure 22: Section from Gastroesophageal junction showing Barrett's oesophagus. With goblet cells. Magnification X100. Stain: Hematoxylin and Eosin.

Intestinal metaplasia has occurred at the gastro-esophageal junction, as defined by the globlet cells present. Intestinal metaplasia is a key indication of Barrett's oesophagus. Goblet cells are characterized by their spherical shape, basal nucleus and spherical apical clear cytoplasm.

http://www.biomedcentral.com/content/pdf/1472-6890-3-5.pdf

3.2 Introduction on Genes

ACBPs are 86-103 residue proteins and were originally isolated from human brain tissue as putative ligands of PBR. They have been characterised and found to be conserved among different species ranging from yeast to mammals (Swinnen J.V. *et al.,* 1998). The principle function of ACBPs is to act as an intracellular carrier-protein for medium to long chain acyl-coA, mediating fatty acid transport to the mitochondrion for ß-oxidation. (Swinnen J.V. *et al.,* 1998). ACBPs are grouped into at least four groups being, 1-ACBP, B-ACBP, T-ACBP, and M-ACBP. The two ACBP genes being focussed on in this study are the 1-ACBP and B-ACBP isoforms.

PBRs are relatively small proteins (18kDa) of 169 amino acids, which have been identified in peripheral tissues and are localised on the outer membrane of the mitochondria. Despite the name, PBRs are not only located in peripheral organs but also present in the CNS. PBR forms part of a trimeric complex with VDAC and ANC (Anholt et al., 1986). PBRs are primarily located on the outer mitochondrial membrane.

ACBPs and PBR arouse great interest because of their association with numerous biological functions including the regulation of cellular proliferation, immunomodulation, regulation of steroidogenesis and apoptosis. In situ hybridisation studies were utilized to elucidate the expression patters of these genes at the mRNA level in oesophageal carcinoma. In situ hybridisation required the generation of probes for the three genes, 1-ACBP, B-ACBP and PBR, and so the aim of this study was to produce 5' and 3' probes for each gene for the increase in specificity and validation of results.

3.2.1 In Situ Hybridization

3.2.1.1 Cloning of 1-ACBP, b-ACBP and PBR into pGEM®-T-Easy

3.2.1.1.1 PCR Primer design for 1-ACBP, b-ACBP and PBR probe synthesis

Forward and reverse primers were designed for each probe utilizing bioinformatics tools by means of the NCBI website; www.ncbi.nlm.nih.gov Primers were designed for the amplification of 5' and 3' probes based on the human gene sequences of 1-ACBP (Accession number, M14200) and B-ACBP (Accession number, BC029526) genes to ensure specificity. These gene sequences are very similar and therefore double expression analysis genes are carried out at 5' and 3' ends to measure expression levels and compare to determine whether similar results is observed, which is expected. One set of primer was sufficient to ensure specificity for PBR (Accession number, M36035). Primer sequences are shown in Table 3.1.

3.2.1.1.2 RT-PCR amplification of 1-ACBP, b-ACBP and PBR

Total mRNA was isolated from a normal human kidney cell line and used as a template for cDNA synthesis using a cDNA synthesis kit (Promega™). The cDNA was used as template for PCR using the specific primers designed (Section 3.2.1), and the gene sequences of interest were amplified and analysed via agarose gel electrophoresis. The expected size fragments were obtained; view figures 25 and 28 for results.

3.2.1.1.3 Cloning of 1-ACBP, b-ACBP and PBR into pGEM®-T-Easy

The five PCR products of all three genes were cloned into pGEM®-T-Easy. Colony PCR was used to screen for positive clones containing the inserts and analysed via gel electrophoresis. Small-scale plasmid isolation was performed from these positive clones using a DNA miniprep kit (Promega™), and analysed via gel electrophoresis.

3.2.1.2 Generation of 1-ACBP, b-ACBP and PBR DIG labelled probes

3.2.1.2.1 Restriction digestion of 1-ACBP, b-ACBP and PBR

The purified plasmid DNA was digested with restriction enzymes EcoR I and Pst I. EcoR I was used to release the inserts from the pGEM-T-Easy® vectors to confirm the inserts cloned were present and analysed on agarose gel electrophoresis, see figures 25, 26 and 27 for results. Pst I was used to linearize the vectors for the purpose of probe synthesis.

3.2.1.2.2 Sequencing analysis of 1-ACBP, b-ACBP and PBR

The purified plasmid samples were also sent for sequencing analysis (Inqaba Biotech®) and M13 forward and reverse primers were utilized. The insert sequences generated by sequence analysis were compared with the human cDNA sequences obtained from the NCBI site, to confirm the inserts cloned into pGEM-T-Easy® were the fragments of interest and also to check for mutations that might have been introduced by *Taq* polymerase. Figures 29 A and Band Figures 30 A and B, demonstrate the sequence alignments of all five probes and shows the inserts cloned were the desired fragments. Theses figures also indicate the few mutations occurring within the gene sequences, and proposed to be those caused by *Taq* polymerase during the PCR reaction. The mutations

ranged between 1-5% and therefore would not influence the specificity of interaction of probe to target nucleic acid.

3.2.1.2.3 Generation of 1-ACBP, b-ACBP and PBR DIG labelled probes

The 5 RNA probes were generated using the nonradioactive digoxigenin – antidigoxigenin labelling system, where digoxigenin (DIG) is a cardenolide steroid isolated from *Digitalis* plants. In each case the functional group chemically linked to the nucleotide, digoxigenin-dUTP, with subsequent incorporation of the nucleotide analogue by polymerase enzymes. High affinity antibody (antidigoxigenin) is specifically directed against the functional group hapten is produced. The incorporated label is then detected

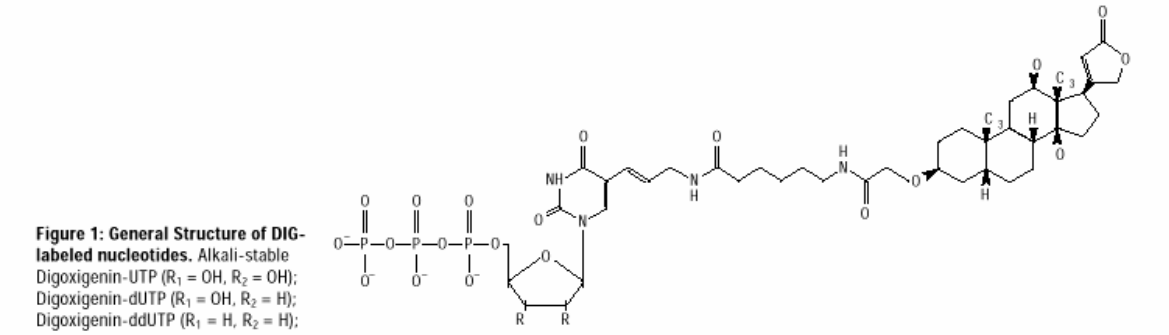

Figure 1: General Structure of DIG-labeled nucleotides. Alkali-stable Digoxigenin-UTP (R_1 = OH, R_2 = OH); Digoxigenin-dUTP (R_1 = OH, R_2 = H); Digoxigenin-ddUTP (R_1 = H, R_2 = H);

with this antibody linked with a colorimetric enzyme.

Figure23: General structure of Dig nucleotides (www.boku.ac.at/zag/text_b.doc).

The probe is detected with chromogenic (colorimetric) substrates and fluorescence.

The colorimetric detection method uses the substrates NBT and BCIP to generate purple/brown precipitate within the cells or nucleus within the tissue.

The following figure shows the reaction when alkaline phosphatase removes the phosphate group of BCIP (5-bromo-4-chloro-3-indolyl-phosphate) the resulting molecules dimerizes under oxidating conditions to give the blue precipitate (5, 5'-dibromo-4,4'-dichloro-indigo). During the reaction with BCIP, NBT (nitroblue tetrazolium) is reduced to its coloured form to give an enhanced colour reaction.

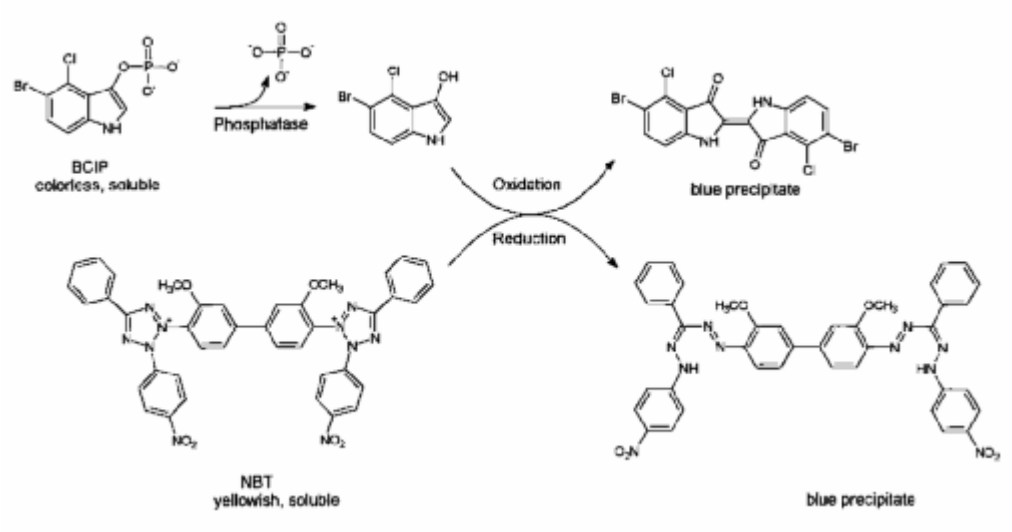

Figure24: Schematic representation of the NBT/BCIP reaction (www.boku.ac.at/zag/text_b.doc)

In the fluorescence method no substrate is added, as the 2º antibody is anti-DIG conjugated to fluorescein isothiocynate (FITC). When excited at a wavelength of 490 nm gives off a bright apple green fluorescence.

Table 20: Primer sets for 1-ACBP, B-ACBP and PBR RT-PCR products

Gene	Primer sequences
1-ACBP 5' Probe	Fwd: **ttgtctgagaccgagctatgtg**
	Rev: **ctcctctgcagctttctcaaac**
1-ACBP 3'Probe	Fwd: **ggatatgagagactggatttgg**
	Rev: **ggtttaacaggttattttcccg**
b-ACBP 5' Probe	Fwd: **gacaacagcagcagcaacaac**
	Rev: **gttctccatcatctggtcttg**
b-ACBP 3' Probe	Fwd: **ttgtcgacggaagatgcgac**
	Rev: **gcctctccctctaaatgttag**
PBR	Fwd: **ttcacagagaaggctgtggttc**
	Rev: **gccatacgcagtagttgagtgt**

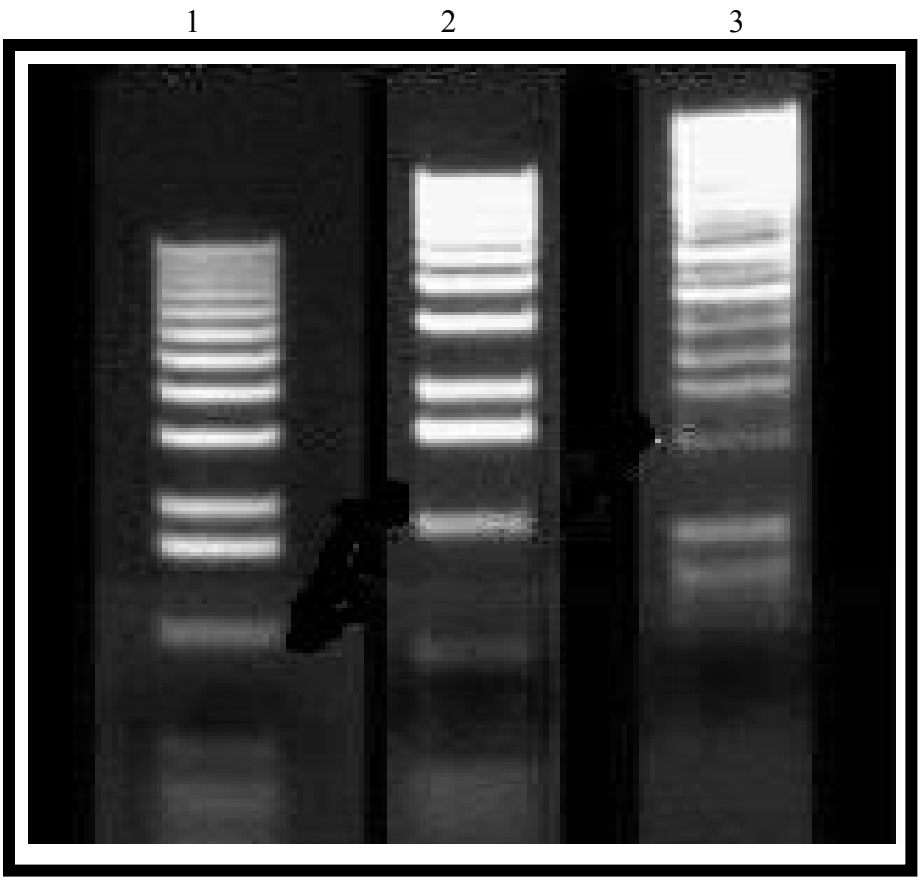

Figure 25: Formaldehyde agarose gel electophoresis of RNA samples.
Lane 1: 7 µl RNA sample mixed with 7µl formaldehyde gel loading buffer (1:1); Lane 2: 10 µl RNA sample mixed with 10µl formaldehyde gel loading buffer; Lane 3: 15 µl RNA sample mixed with 15µl formaldehyde gel loading buffer. The gel was electrophoresed with 1X MOPS at 50 V for 1 hour.

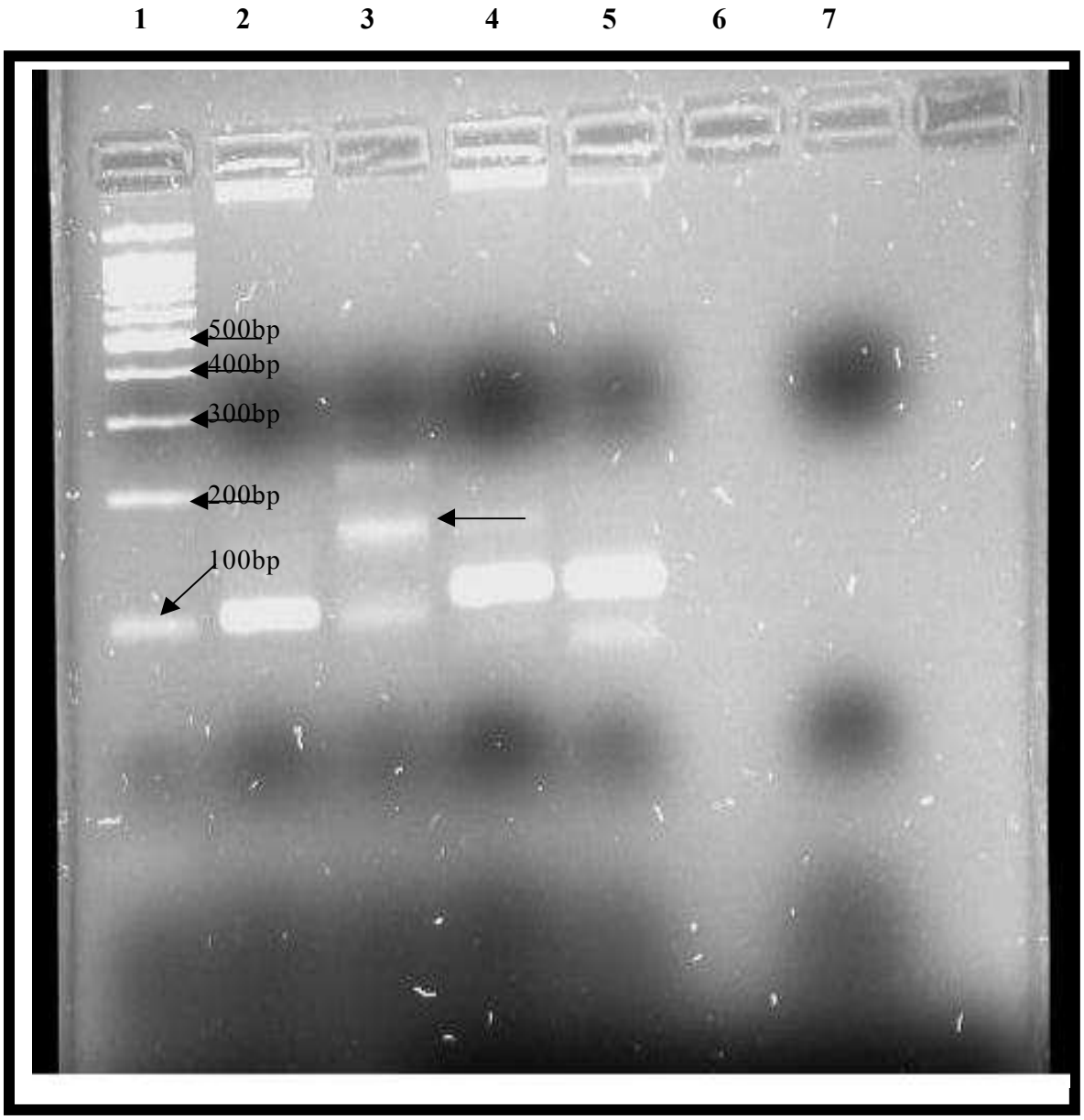

Figure 26: 0.8% Agarose gel electrophoresis of 1-ACBP and B-ACBP RT-PCR products

Lane 1: 100bp Molecular weight marker; Lane 2: 5' 1-ACBP; Lane 3: 5' B-ACBP; Lane 4: 3'1-ACBP; Lane 5: 3' B-ACBP, Lane 7: Negative control (H_2O). The gel was run for 1 hour at 200 V.

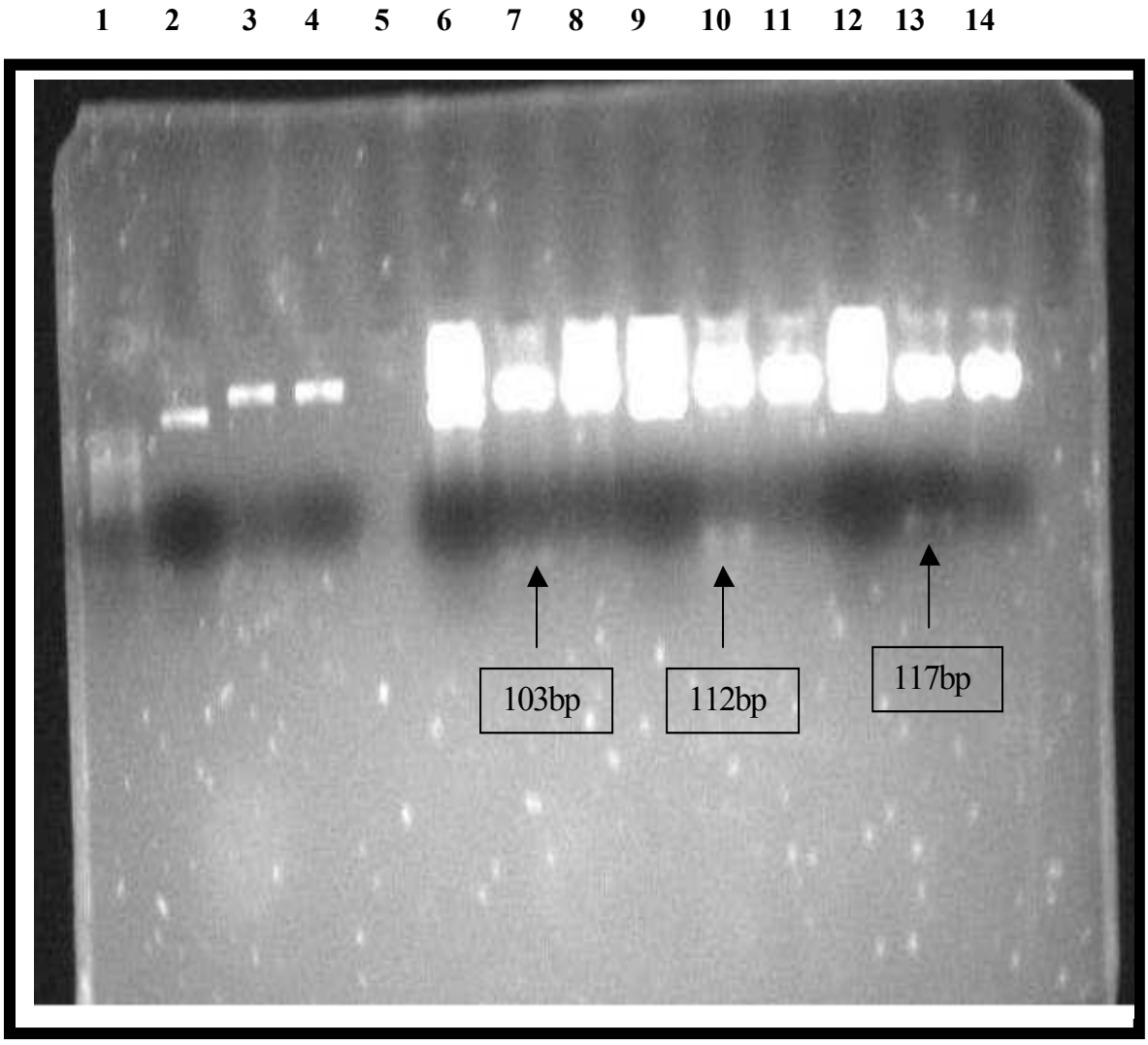

Figure 27: 0.8% Agarose gel electrophoresis of restriction digestions.

Lane1: 100bp Molecular weight marker; Lane 6: 5' 1ACBP clone; Lane 7: 5' 1-ACBP clone digested with EcoRI; Lane 8: 5' 1-ACBP clone cut with PST I; Lane 9: 5' B-ACBP Clone; Lane 10: 5' B-ACBP clone cut with EcoRI; Lane 11: 5' 1-ACBP clone cut with PST I; Lane 12: 3' 1-ACBP clone; Lane 13: 3' 1-ACBP clone cut with EcoRI; Lane 14: 3' 1-ACBP clone cut with PST I. The gel was run at 200V for 1 hour.

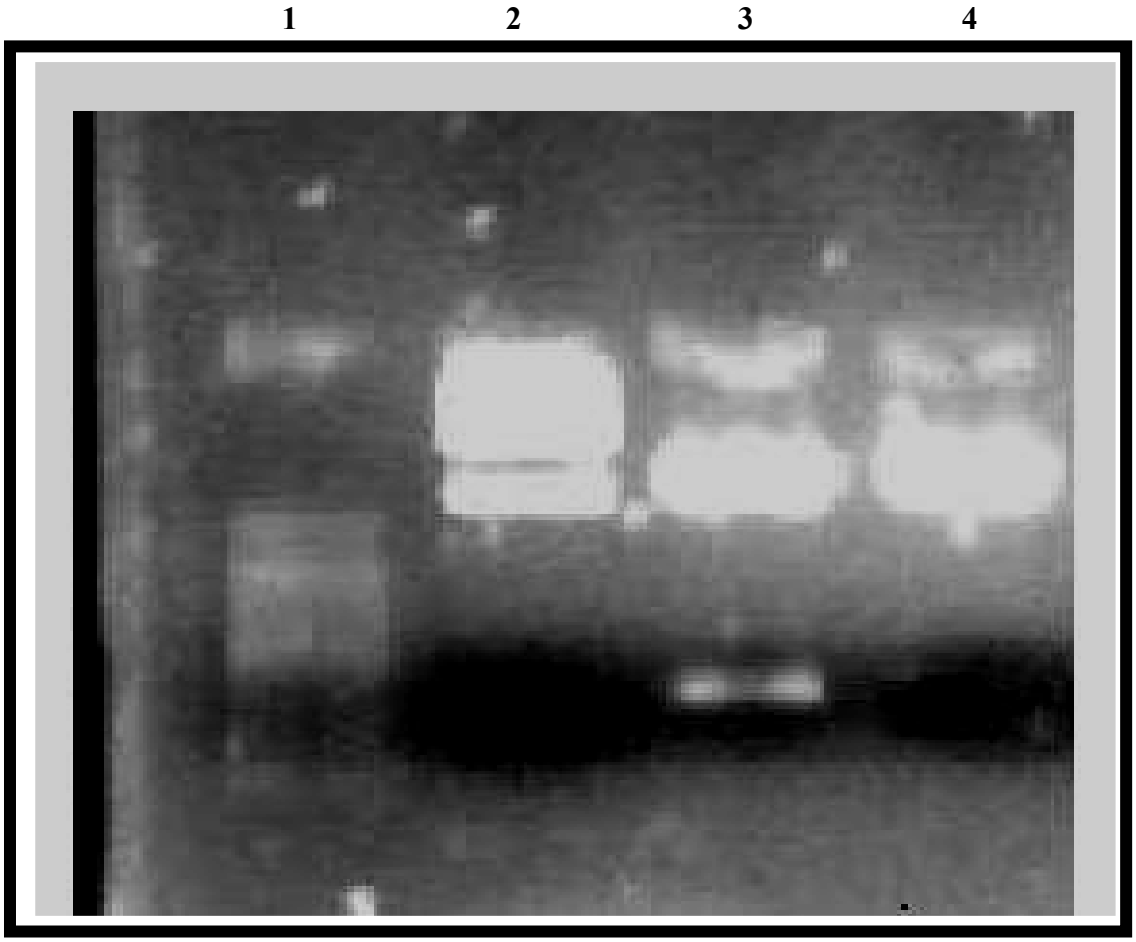

Figure 28: 0.8% Agarose gel electrophoresis of restriction digests.

Lane 1: 100bp Molecular weight marker; Lane 2: 3' B-ACBP clone; Lane 3: 3' B-ACBP clone digested with EcoRI; Lane 4: 3 B-ACBP clone digested with Pst I. The gel was run at 200V for 1 hour.

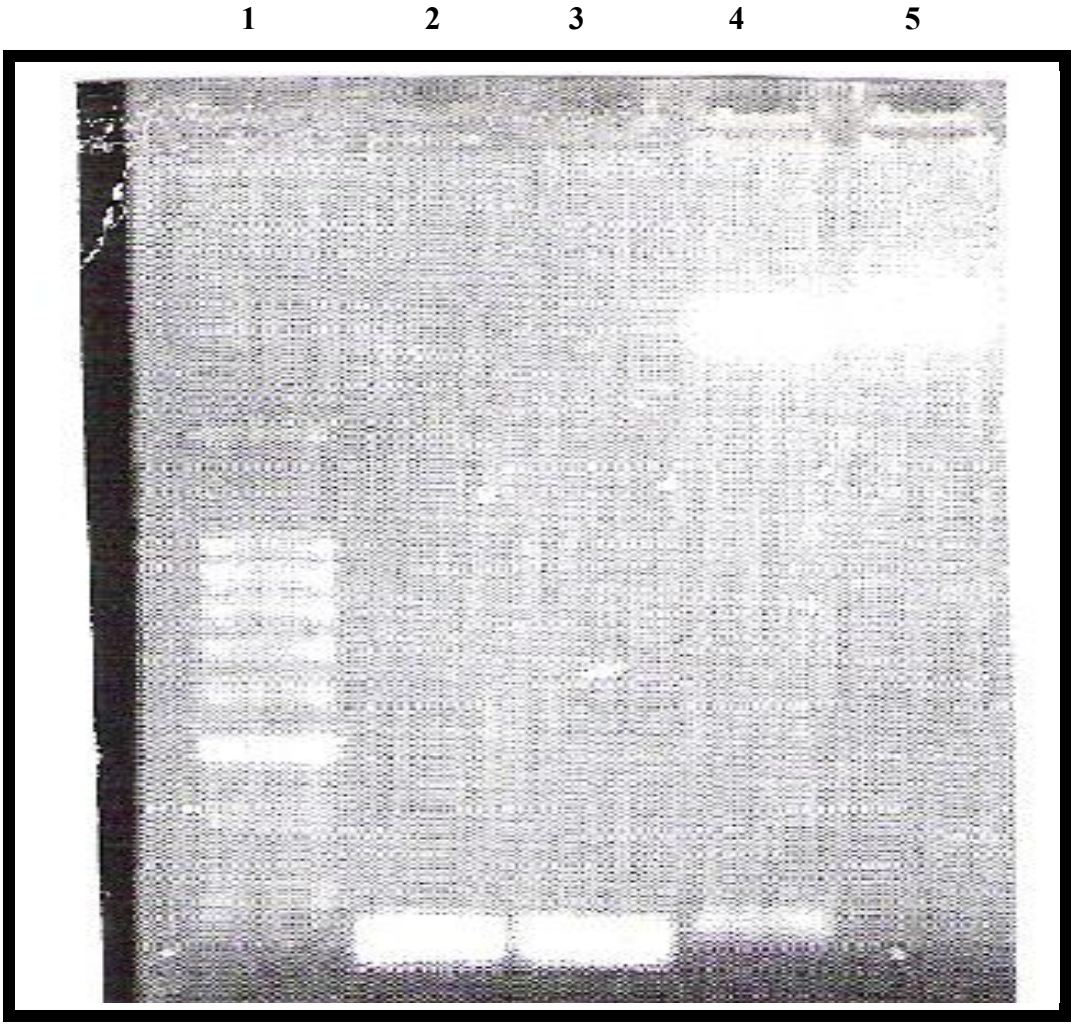

Figure 29: 0.8% Agarose gel electrophoresis of PBR RT PCR and restriction digest products

Lane 1: 100bp molecular weight marker. Lane 2: RT-PCR product; Lane 3: Colony PCR; Lane 4: EcoRI restriction digest; Lane 5: Pst I restriction digest. The gel was run at 180V for 1hour.

Figure 30: Sequencing results of the two 1-ACBP inserts

A:

3' 1-ACBP insert

```
Query: 95  tggtttaacaggttattttcccgaattcccaccatccacggtattagnnnnnnncaaggc 154
           |||||||||  ||||||||||||||||||||||||||||||||||       ||||||
Sbjct: 444 tggtttaactggttattttcccgaattcccaccatccacggtattagaaaaaaacaaggc 385


Query: 155 attgtctcagtttaggataaacacatggcacagtaaccaaatccagtctctcatatcc 212
           ||||||||||||||||||||||||||||||||||||||||||||||||||||||||||
Sbjct: 384 attgtctcagtttaggataaacacatggcacagtaaccaaatccagtctctcatatcc 327
```



B:

5' 1-ACBP insert

```
Query: 3   ttgtctgagaccgagctatgtggggcgacctctggctcctcccgcctgcctctgccaatc 62
           |||||||||||||||||||||||||||||||||||||||||||||||||||||||||| |||
Sbjct: 153 ttgtctgagaccgagctatgtggggcgacctctggctcctcccgcctgcctctgcctatc 94


Query: 63  cgggcactgggacagaggctgagtttgagaaagctgcagaggag 106
           |||||||||||||||||||||||||||||||||||||||||||
Sbjct: 93  cgggcactgggacagaggctgagtttgagaaagctgcagaggag 50
```



Figure 31: Sequencing results of the 2 B-ACBP inserts

A:

5' B-ACBP insert

```
Query: 73  gttctccatcatctggtcttgctttcagcttcctcacatcttctgcagccctgtcaaaat 132
           ||||||||||||||||||||||||||||||||||||||||||||||||||||||||||||
Sbjct: 124 gttctccatcatctggtcttgctttcagcttcctcacatcttctgcagccctgtcaaaat 65


Query: 133 cagcctgcagggccatggtggcggctgccgcgttgttgctgctgctgttgtc 184
           |||||||||||||||||||||||||||||||||||||||||||||||||||
Sbjct: 64  cagcctgcagggccatggtggcggctgccgcgttgttgctgctgctgttgtc 13
```



B:

3'B-ACBP Probe

```
Query: 244 ttgtcgacggaagatgcgacgagtgcctatatttctaaagcaaaggagctgatag-aaaa 302
           |||||||||||||||||||||||||||||||||||||||||||||||||||||| ||||
Sbjct: 92  ttgtcgacggaagatgcgacgagtgcctatatttctaaagcaaaggagctgatagtaaaa 151


Query: 303 atacggaatttagaatacagcatatgaggaatttttccttttgaagacttccaaatgcta 362
           ||||||||||||||||||||||||||||||||||||||||||||||||||||||||||||
Sbjct: 152 atacggaatttagaatacagcatatgaggaatttttccttttgaagacttccaaatgcta 211


Query: 363 tcatgacctaacatttagagggagaggca 391
           |||||||||||||||||||||||||||||
Sbjct: 212 tcatgacctaacatttagagggagaggca 240
```



Figure 32: Sequencing results of the PBR insert



```
Query: 89  ttcacagagaag-ctgtggttcccctgggcctctacactgggcagctggccctgaactgg 147
           |||||||||||| ||||||||||||||||||||||||||||||||||||||||||||||
Sbjct: 220 ttcacagagaaggctgtggttcccctgggcctctacactgggcagctggccctgaactgg 279


Query: 148 gcatggccccccatcttctttggtgcccgacaaatgggctgggccttggtggatctcctg 207
           |||||||||||||||||||||||||||||||||||||||||||||||||||||||||||
Sbjct: 280 gcatggccccccatcttctttggtgcccgacaaatgggctgggccttggtggatctcctg 339


Query: 208 ctggtcagtggggcggcggcagccactaccgtggcctggtaccaggtgagcccgctggcc 267
           |||||||||||||||||||||||||||||||||||||||||||||||||||||||||||
Sbjct: 340 ctggtcagtggggcggcggcagccactaccgtggcctggtaccaggtgagcccgctggcc 399


Query: 268 gcccgcctgctctacccctacctggcctggctggccttcgcgaccacactcaactactgc 327
           |||||||||||||||||||||||||||||||||||||||||||||||||||||||||||
Sbjct: 400 gcccgcctgctctacccctacctggcctggctggccttcgcgaccacactcaactactgc 459
```

3.2.1.3 Localization of 1-ACBP, B-ACBP and PBR mRNAs in oesophageal tissue

3.2.1.3.1 Colorimertric In Situ Hybridization

3.2.1.3.1.1 Results of 3' 1-ACBP probe:

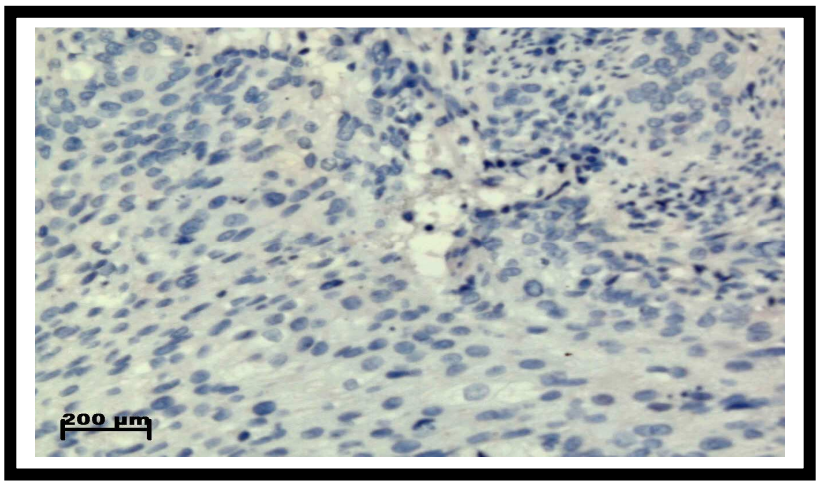

(A)

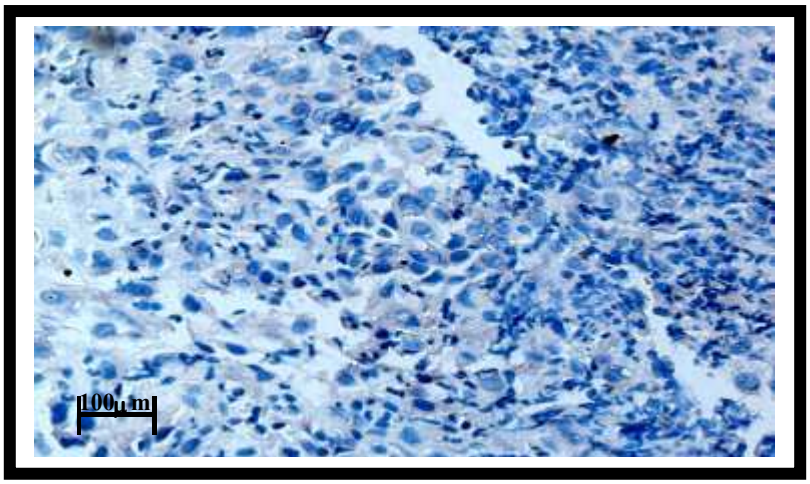

(B)

Figure 33: Experimental controls for ISH, on invasive squamous carcinoma of the oesophagus

(A) Negative control containing water on a high grade, invasive squamous cell carcinoma tissue section, with fat cells in the centre right, and as expected no localisation occurred. (B) 3'-1-ACBP sense strand control on a high-grade dysplastic tissue section, also showing no localization as expected. Magnification X400. Stain: NBT/BCIP and Hematoxylin counterstain.

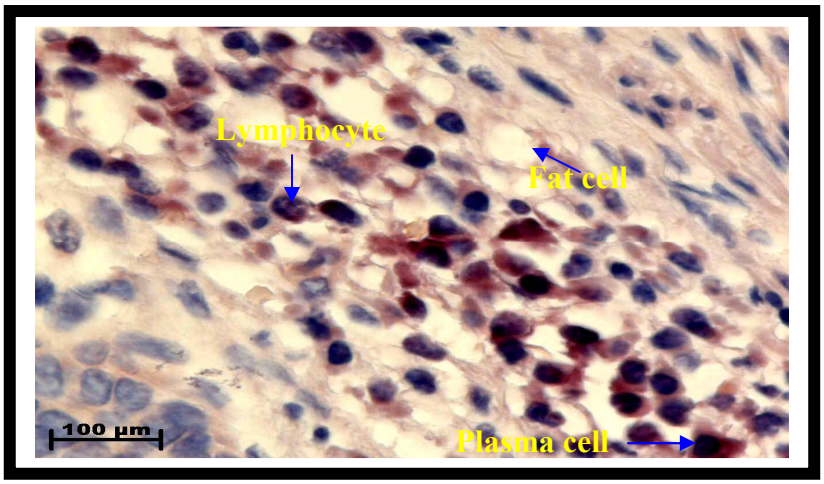

(A)

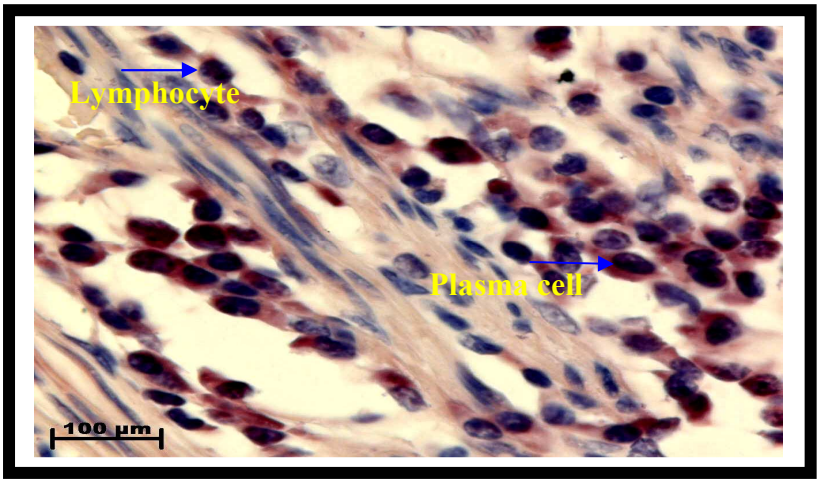

(B)

Figure 34: Localisation of 3'1-ACBP in moderately differentiated squamous cell carcinoma of the oesophagus.

(A) The micrograph illustrates an adipose tissue section in the adventitia of a high-grade squamous cell carcinoma of the oesophagus. The 3'1-ACBP probe localises to the cytoplasm of mostly plasma cells (cell with eccentric nucleus), and a few lymphocytes (smallest cell with no obvious cytoplasm surrounding it), in the fat cells. (B) In between the skeletal muscle layer of an infiltrating moderately differentiated squamous cell carcinoma, the 3'1-ACBP probe also localises to plasma cells, and a few lymphocytes, but no localisation occurs in the fibroblasts of the skeletal muscle. Magnification X1000. Stain: NBT/BCIP and Hematoxylin counterstain.

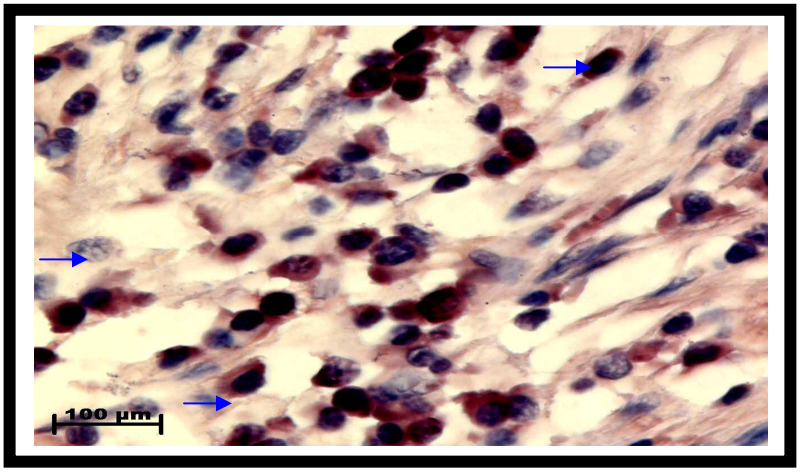

(A)

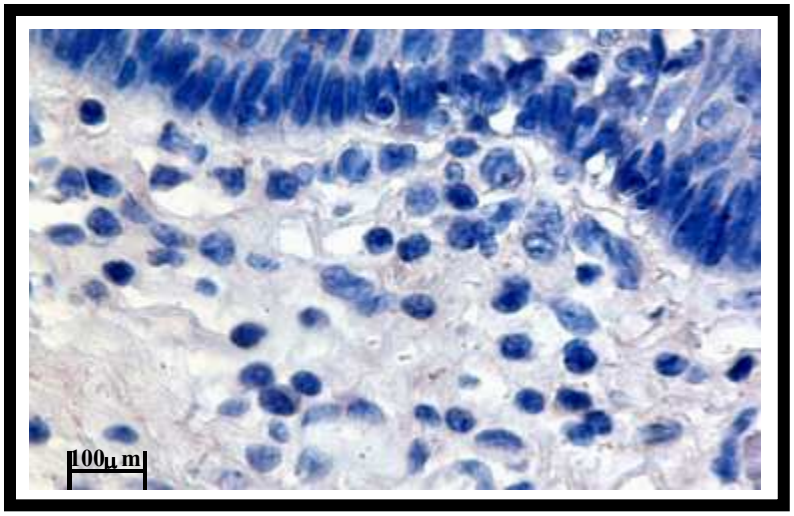

(B)

Figure 35: 3'1-ACBP localization on diseased and normal lamina propria

(A) 3'1-ACBP probe was highly expressed in plasma cells in the lamina propria of a well-differentiated, high-grade squamous cell carcinoma of the oesophagus. (B) 3'1-AC probe showed no localization within the lamina propria of normal oeosphageal tissue sections as indicated by the arrows pointing to the cytoplasm of a plasma cell. Magnification X1000. Stain: NBT/BCIP and Hematoxylin counterstain.

3.2.1.3.1.2 Results of 5'1-ACBP probe:

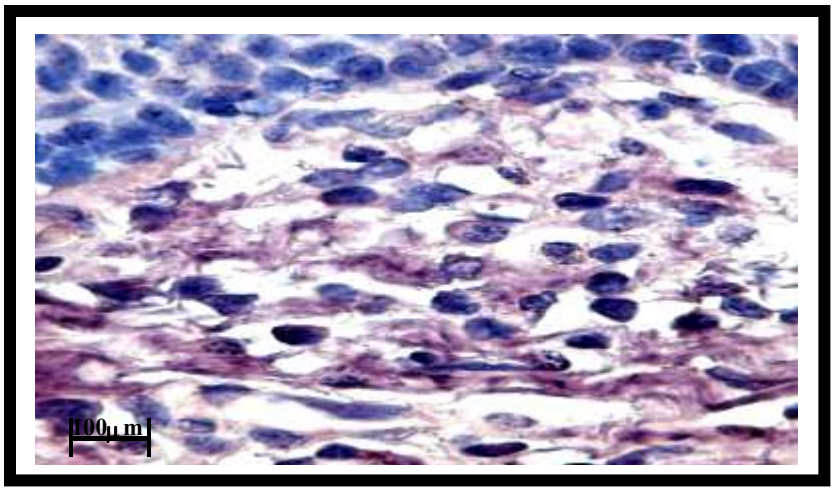

(A)

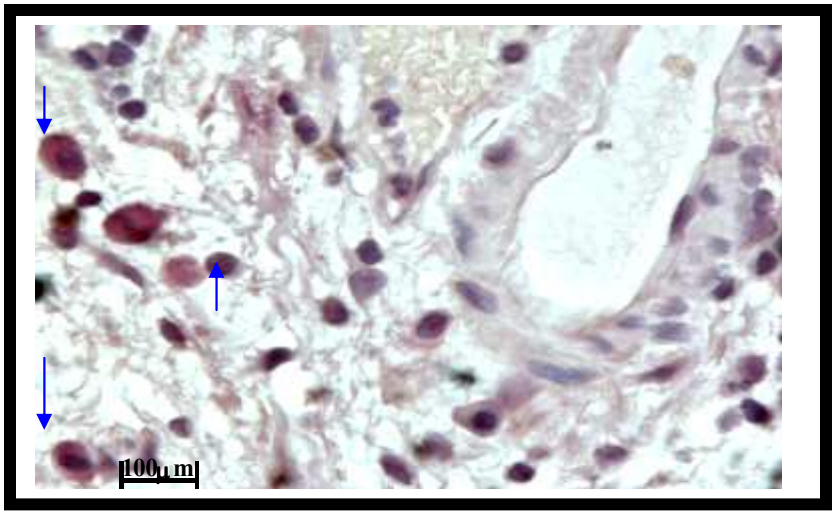

(B)

Figure 36: 5'1-ACBP localization within the submucosa

(A) 5'1-ACBP is localized to the lamina propria of well differentiated low grade squamous carcinoma, showing an upregulation of the gene in plasma cells and lymphocytes (B) In this micrograph 5'1-ACBP mRNA probe localizes in the submucosa with nuclear localization occurring in plasma cells macrophage (cell with nucleus in centre and cytoplasm surrounding it), and low expression in few lymphocytes. This is a well-differentiated squamous carcinoma with a high grade of dysplasia. Magnification X1000. Stain: NBT/BCIP and Hematoxylin counterstain.

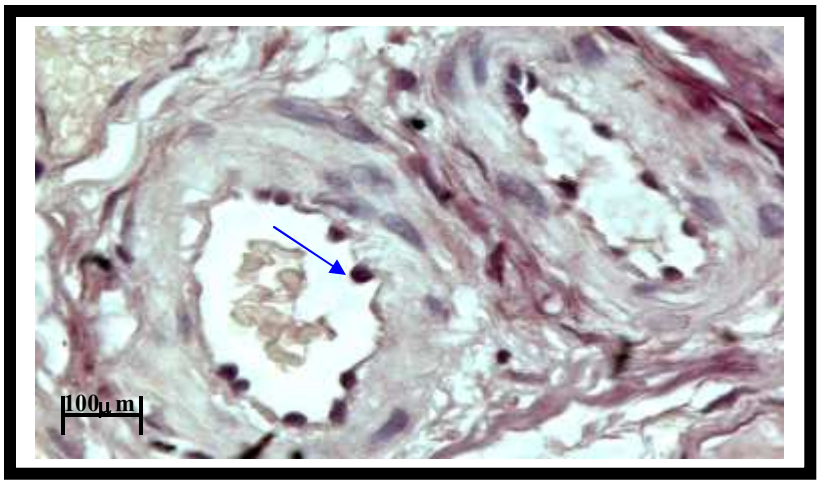

(A)

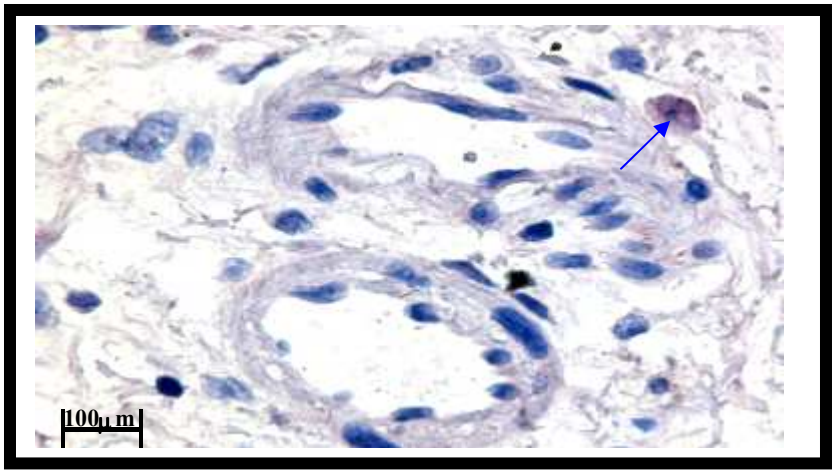

(B)

Figure 37: 5'1-ACBP localization to diseased and normal arteries in submucosa

(A) 5'1-ACBP localizes in the connective tissue of well a differentiated low-grade dysplasia oesophageal section. Here an increase in expression occurs in the endothelial cells in the inner lining of arteries wall, no localization occurs in the fibroblasts of the artery. (B) Here 5'1-ACBP does not localize to any endothelial cells in the normal oesophagus, except to the cytoplasm of a mononuclear mast cell. Magnification X1000. Stain: NBT/BCIP and Hematoxylin counterstain.

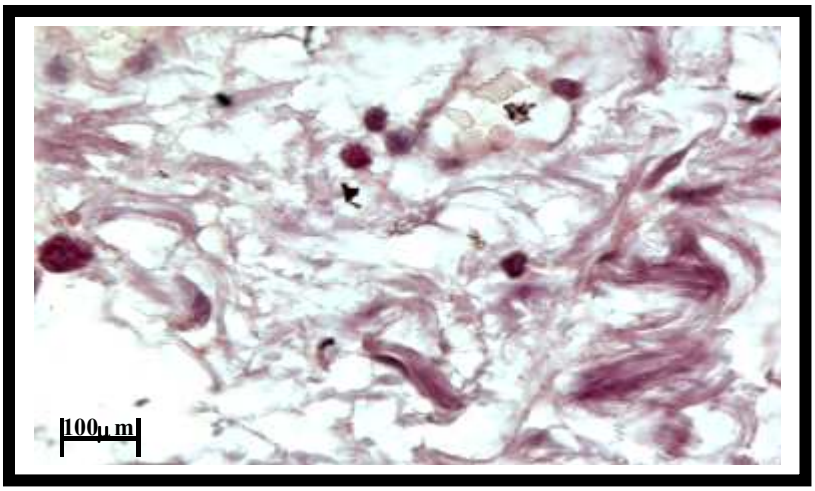

(A)

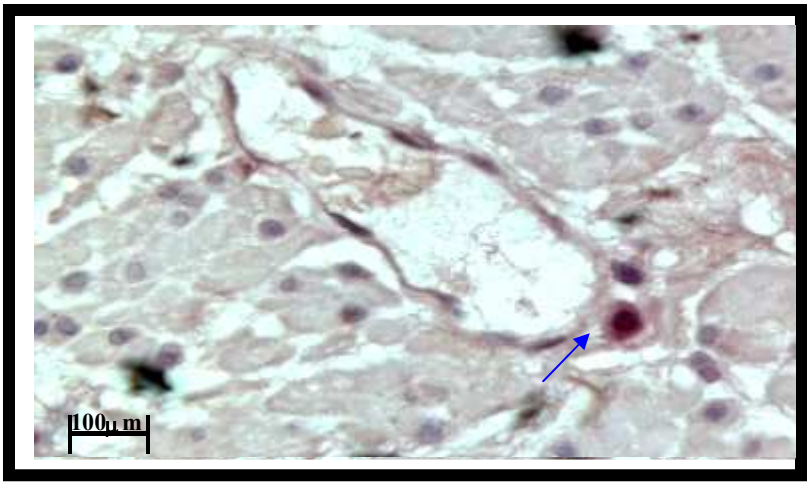

(B)

Figure 38: 5'1-ACBP in connective tissue and submucosa of diseased tissue.

(A) 5'1-ACBP is upregulated within connective tissue of the diseased oesophagus, and localizes to neutrophils and lymphocytes here. (B) 5'1-ACBP localizes to a monocyte in the submucosa of a well-differentiated, high-grade squamous carcinoma. Magnification X1000. Stain: NBT/BCIP and Hematoxylin counterstain.

3.2.1.3.1.3 Results of 3'B-ACBP probe:

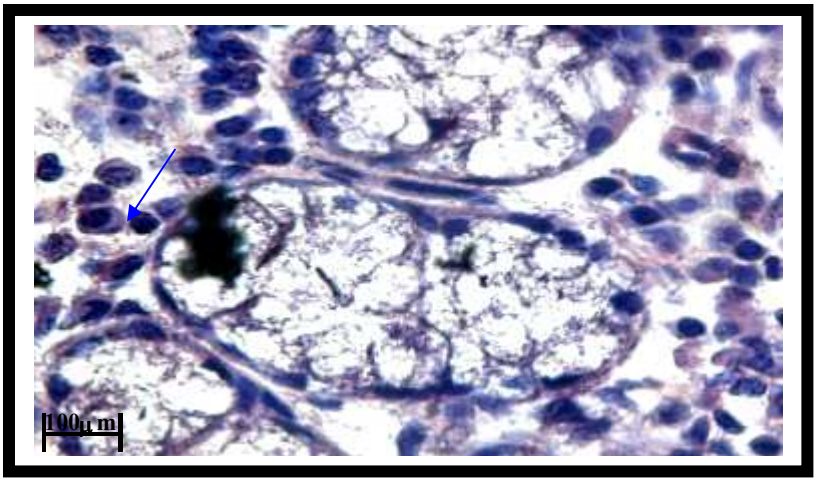

(A)

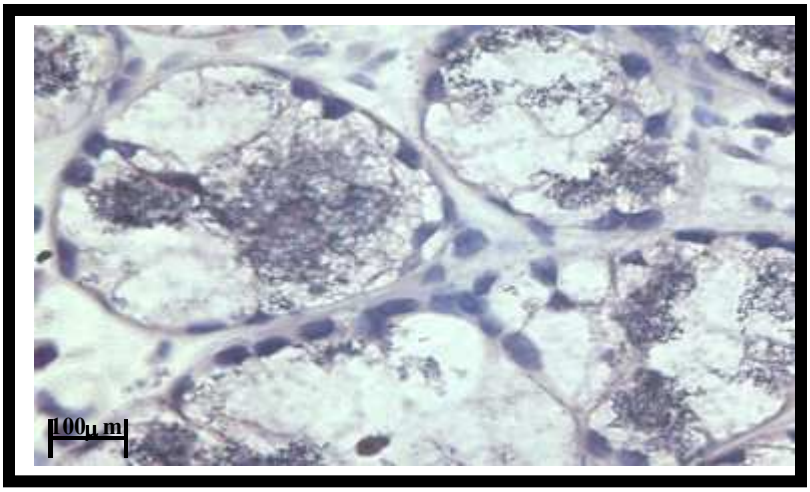

(B)

Figure 39: 3'B-ACBP localization to diseased and normal oesophageal tissue

(A) This micrograph represents the localization of 3'B-ACBP in plasma cells in a low-grade dysplastic squamous cell carcinoma, and an intermediate expression level of the gene is detected. (B) This micrograph represents a normal oesophageal tissue section and no localization of 3'BACBP is detected here. Magnification X1000. Stain: NBT/BCIP and Hematoxylin counterstain.

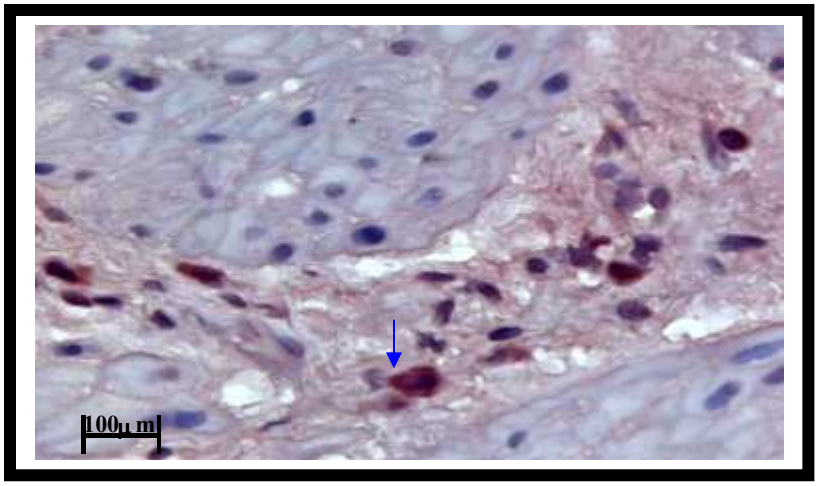

(A)

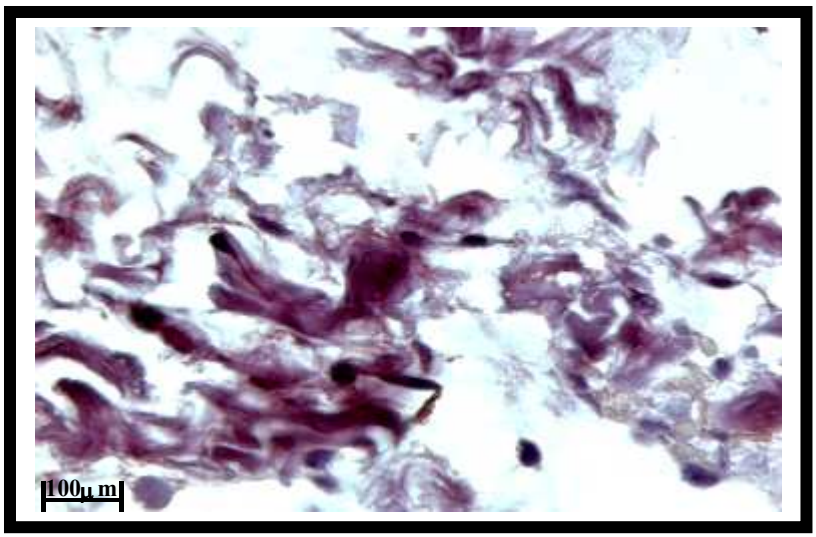

(B)

Figure 40: Localization within the muscularis externa of the diseased oesophagus

(A) Localization occurs within plasma cells and lymphocytes in the longitudinal muscle layer of a moderately well differentiated high-grade squamous carcinoma and is upregulated compared to the normal oesophageal longitudinal muscle layer. (C) Upregulation of the 3'B-ACBP probe is seen in the connective tissue of a high-grade dysplasia squamous carcinoma tissue section as well. Magnification X1000. Stain: NBT/BCIP and Hematoxylin counterstain.

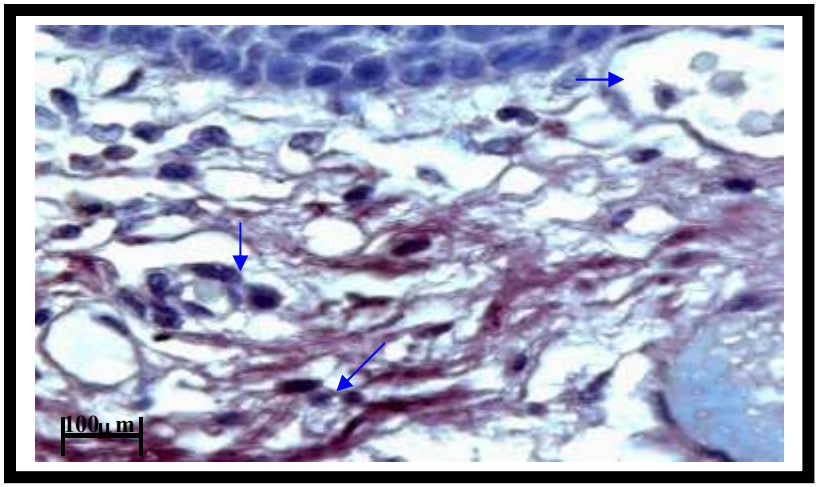

(A)

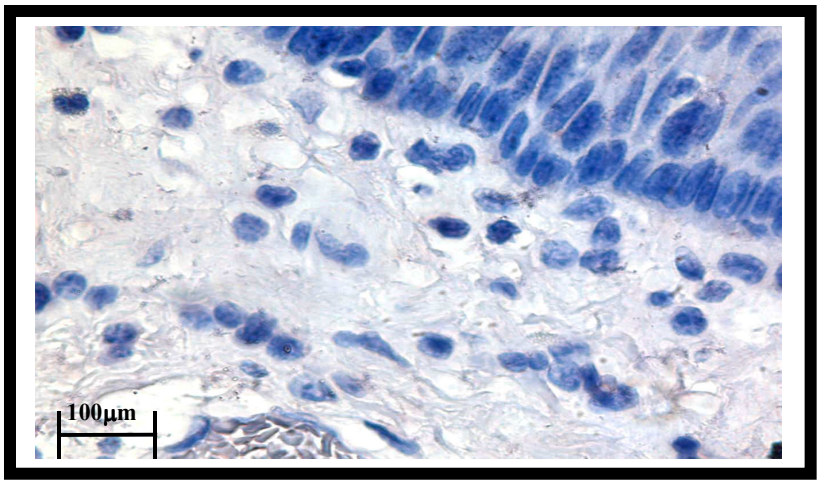

(B)

Figure 41: 3'B-ACBP localization in diseased and normal lamina propria

(A) 3'B-ACBP is upregulated in a moderately well differentiated high-grade squamous carcinoma, with localization occurring in plasma cells, lymphocytes and macrophages. (B) This is a normal oesophageal tissue section and no localization occurs within this section of the oesophagus. Magnification X1000. Stain: NBT/BCIP and Hematoxylin.

3.2.1.3.1.4 5'B-ACBP probe results

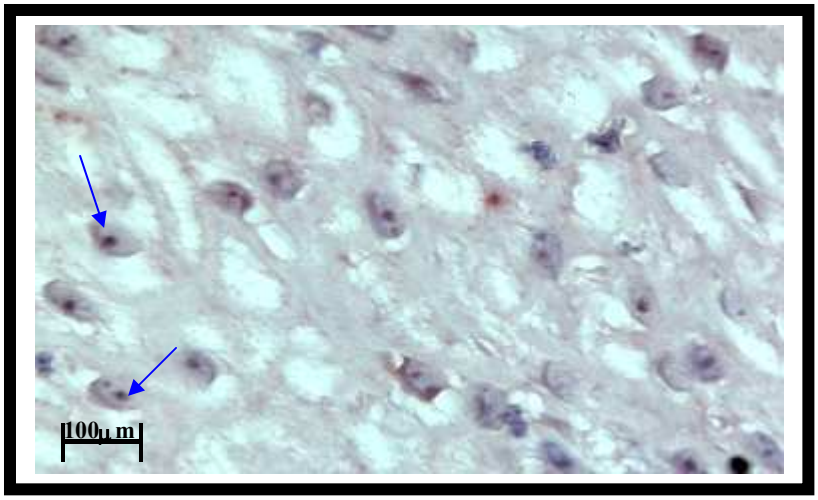

(A)

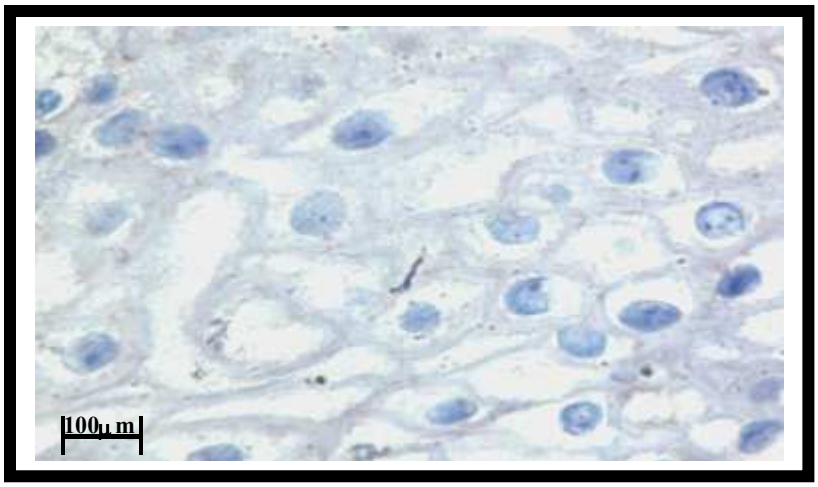

(B)

Figure 42: Comparative analysis of 5'B-ACBP in diseased and normal epithelium

(A) Localization occurs within the nucleus of epithelial cells of a low-grade dypslatic tissue section. (B) Negative control containing water on a low-grade dysplastic tissue sample of the oesophagus, showing no localization within the epithelial cells. Magnification X1000. Stain: NBT/BCIP and Hematoxylin counterstain.

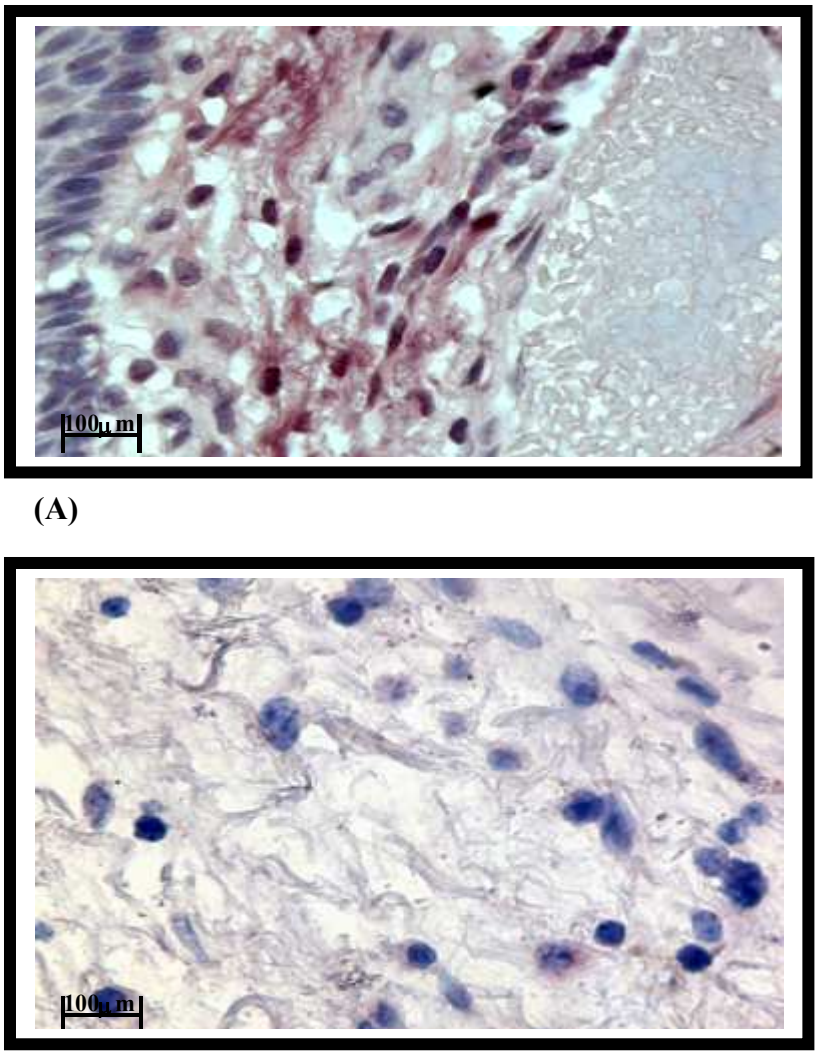

Figure 43: 5'B-ACBP localization in diseased and normal lamina propria

(A) In the lamina propria of a high-grade dysplastic squamous carcinoma tissue sample of the oesophagus, 5'B-ACBP localizes to the cytoplasm of the lymphocytes and plasma cells as well. (B) Lamina propria section of the normal oesophagus shows no to very low localization of the 5'B-ACBP probe. Magnification X1000. Stain: NBT/BCIP and Hematoxylin counterstain.

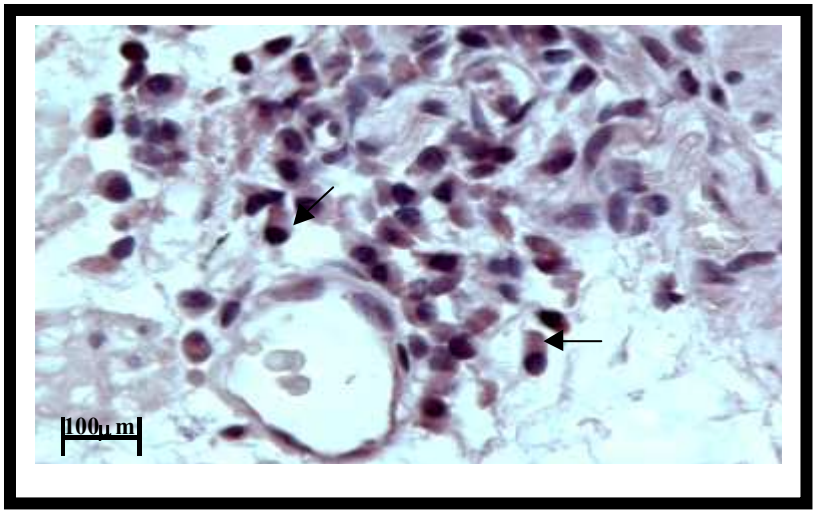

(A)

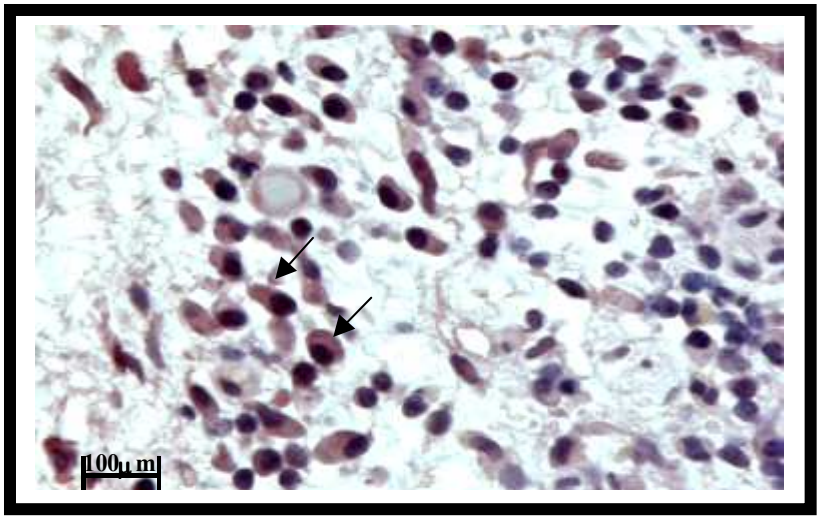

(B)

Figure 44: Colorimetric in situ hybridization results of 5'B-ACBP:

(A) The 5'B-ACP probe localizes mainly to plasma cells in the connective tissue section of the submucosa of a moderately well differentiated high-grade dysplatic tissue sample of the oesophagus. (B) An upregulation of 5'B-ACBP occurs within the lamina propria of a well-differentiated high-grade dysplastic tissue sample of the oesophagus. Magnification X1000. Stain: NBT/BCIP and Hematoxylin counterstain.

3.2.1.3.1.5 PBR probe results:

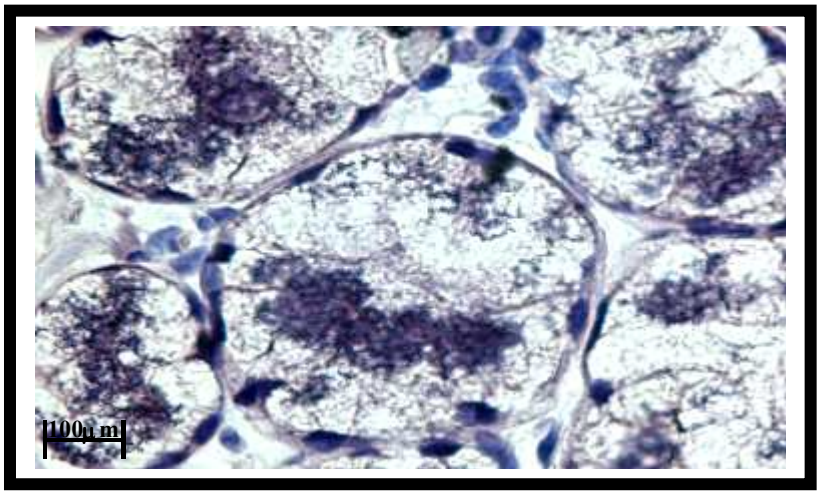

(A)

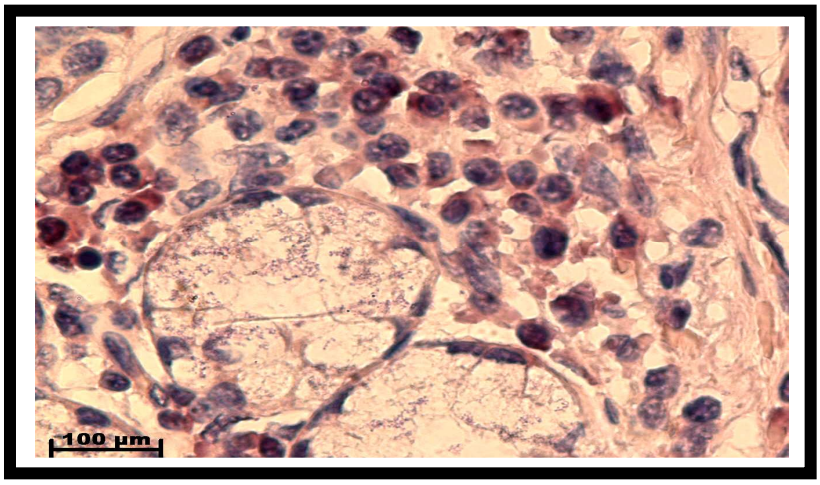

(B)

Figure 45: PBR localization within the Mucous acini glands in diseased and normal oesophageal tissue sections.

A) Upregulation of the PBR mRNA is found around the mucous acini glands in the connective tissue section of the submucosa, in a high-grade invasive squamous carcinoma. It localizes to the cytoplasm of plasma cells and lymphocytes as well. (B) This is mucous acini glands of a normal oesophagus tissue section, and no PBR localization is found around these glands. Magnification X1000. Stain: NBT/BCIP and Hematoxylin counterstain.

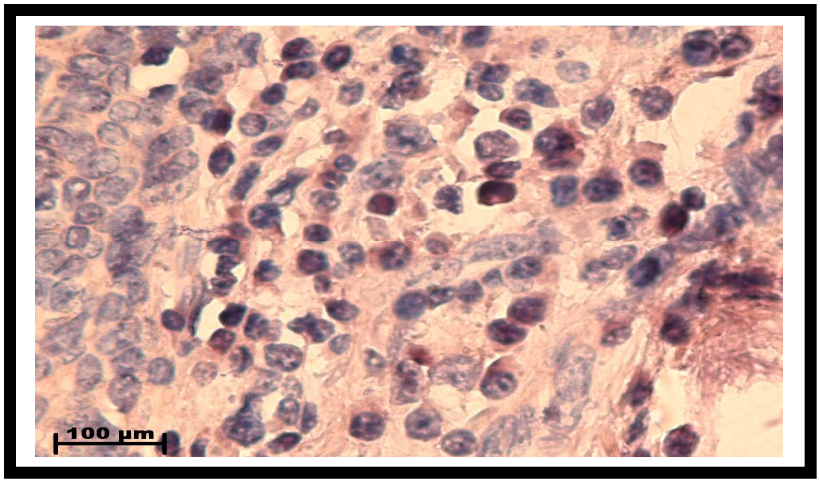

(A)

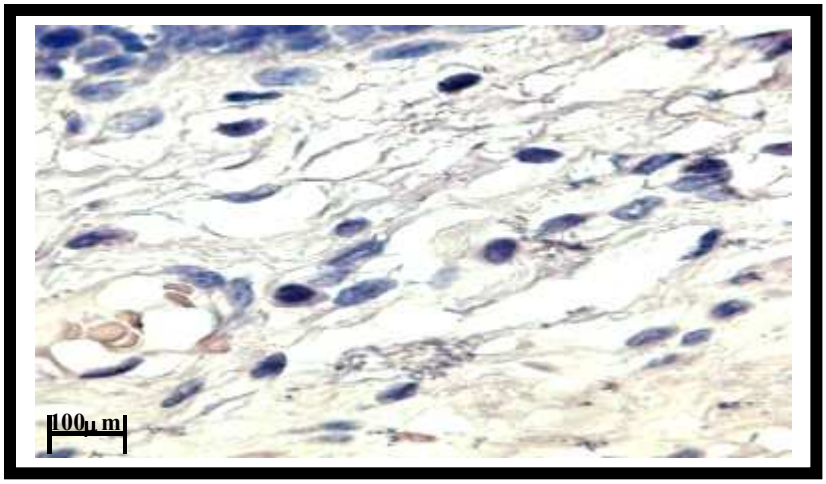

(B)

Figure 46: PBR localization within diseased and normal lamina propria

(A) In the lamina propria of a high-grade invasive squamous carcinoma, plasma cells and few lymphocytes localization occurs. (B) This is a lamina propria section of the normal oesophagus and no PBR localization is found. Magnification X1000. Stain: NBT/BCIP and Hematoxylin counterstain.

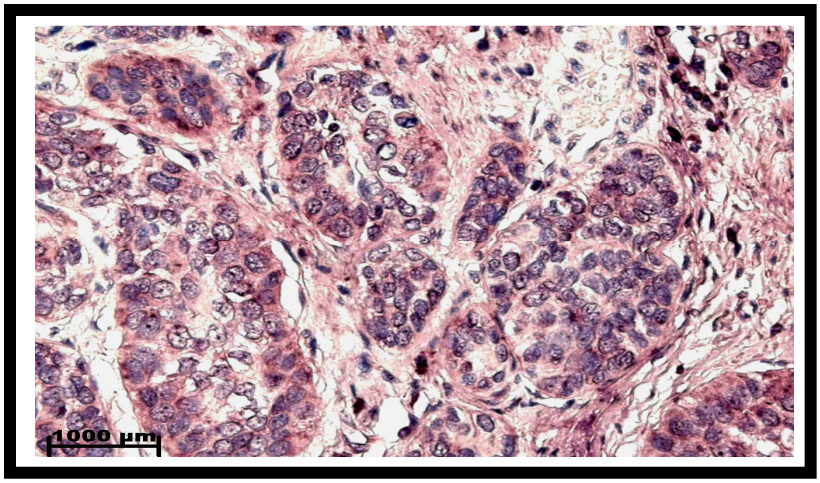

(A)

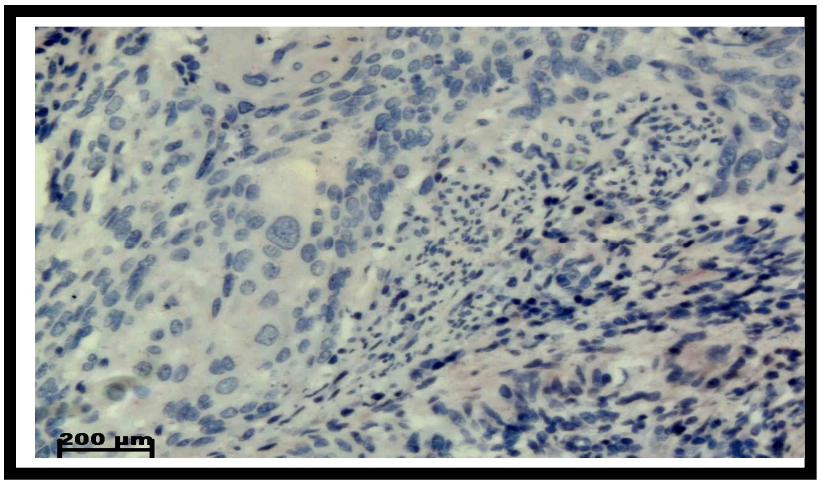

(B)

Figure 47: PBR localization in an invasive squamous carcinoma tissue section

(A) This micrograph shows tumour islands in the stroma of an invasive squamous carcinoma. PBR is expressed in the tumour islands but not in the nucleus of the tumour cells. (B) This micrograph represents the localization of the sense strand of PBR, and as expected the experimental control yields no localization. Magnification X1000. Stain: NBT/BCIP and Hematoxylin counterstain.

3.2.1.3.2 Fluorescent In situ Hybridization results:

3.2.1.3.2.1 5’ 1-ACBP Fluorescent ISH results

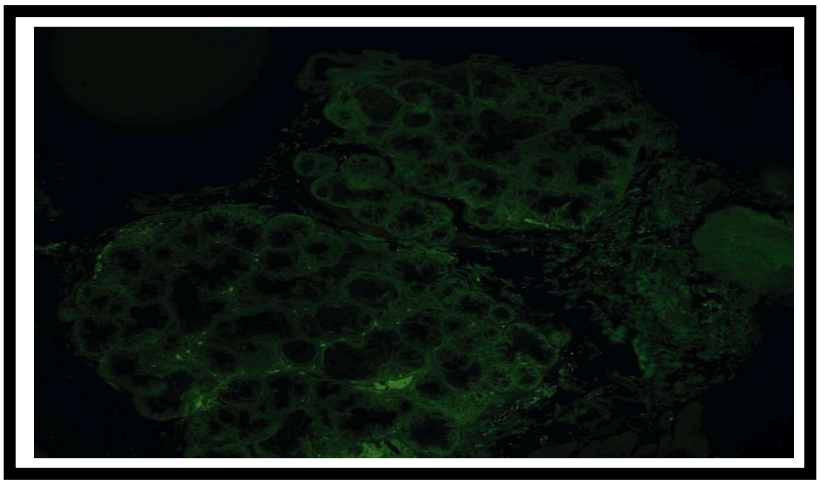

(A)

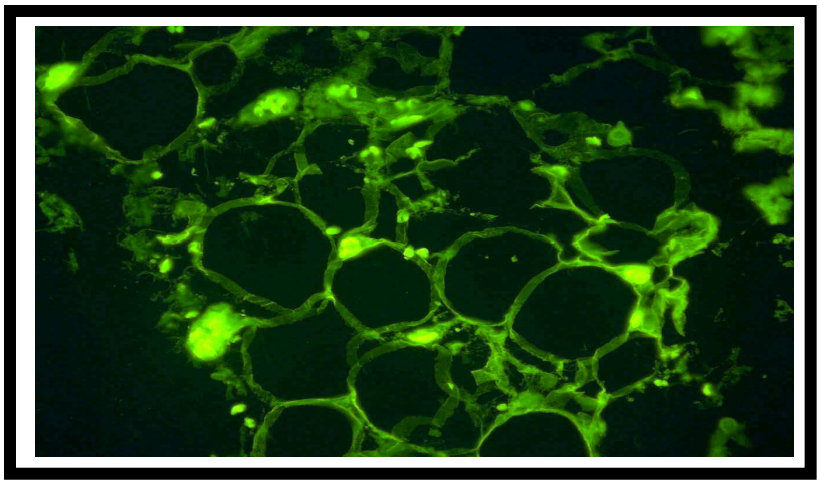

(B)

Figure 48: Fluorescent in situ hybridization results of 5’1-ACBP

(A) This is a negative control of a sense strand of the 5’1ACBP probe on the mucini glands in a low grade dysplastic tissue sample of the oesophagus. (B) 5’1-ACBP localization is found to be upregulated in fat cells of a high-grade dysplastic tissue sample. Magnification X400.

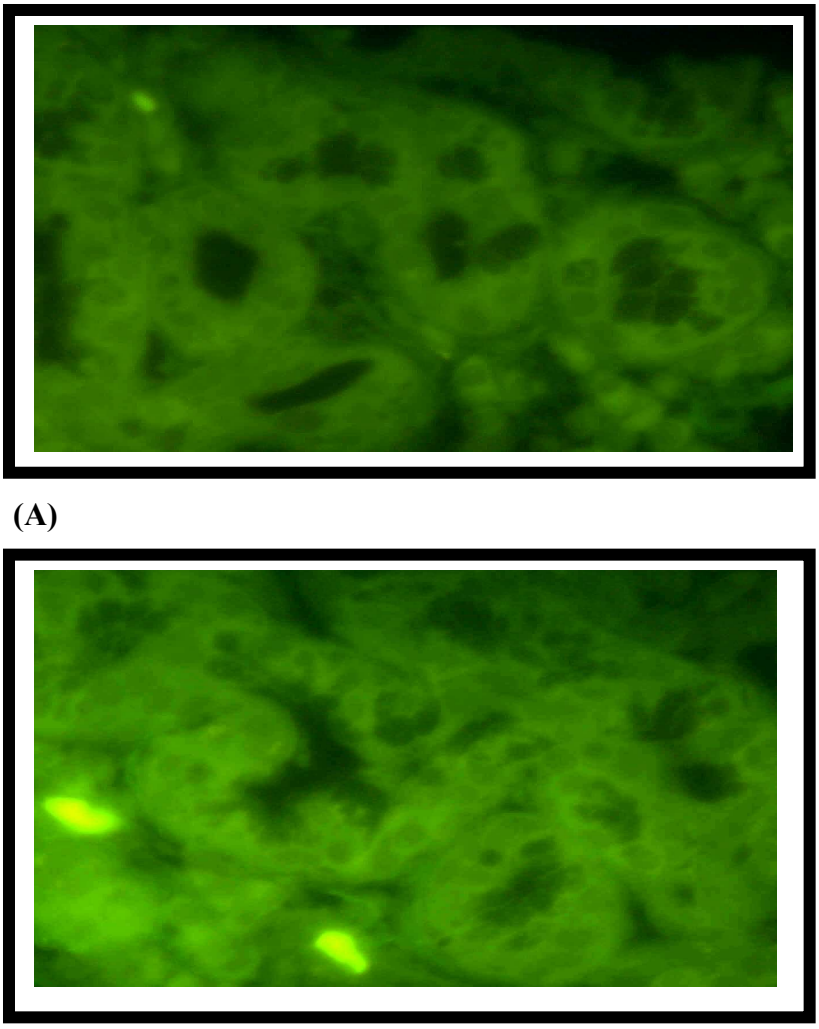

(A)

(B)

Figure 49: Localization of 1-ACBP in mucini glands in the submucosa

(A) Mucous acini glands in the connective tissue section of the submucosa of the normal oesophagus, where nearly no localization occurs. (B) Mucous acini glands in a high-grade dysplastic squamous carcinoma tissue sample of the oesophagus, shows an increase in expression of the 1-ACBP gene. Magnification X400.

3.2.1.3.2.2 3’ B-ACBP fluorescent ISH results:

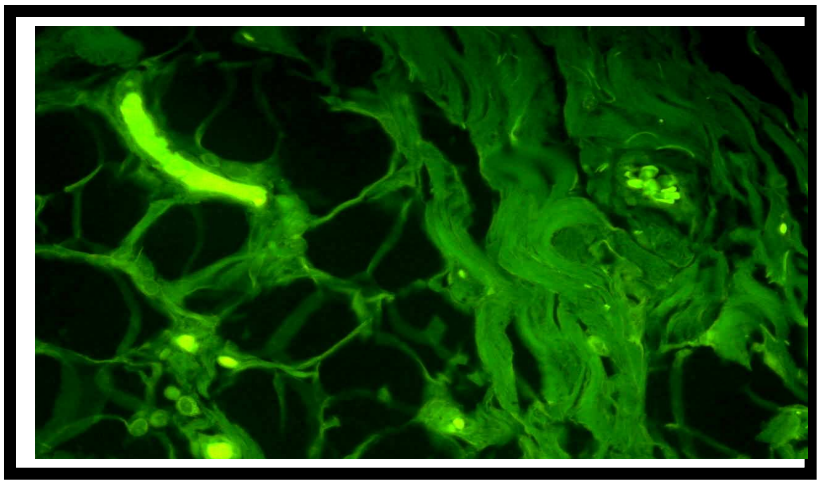

(A)

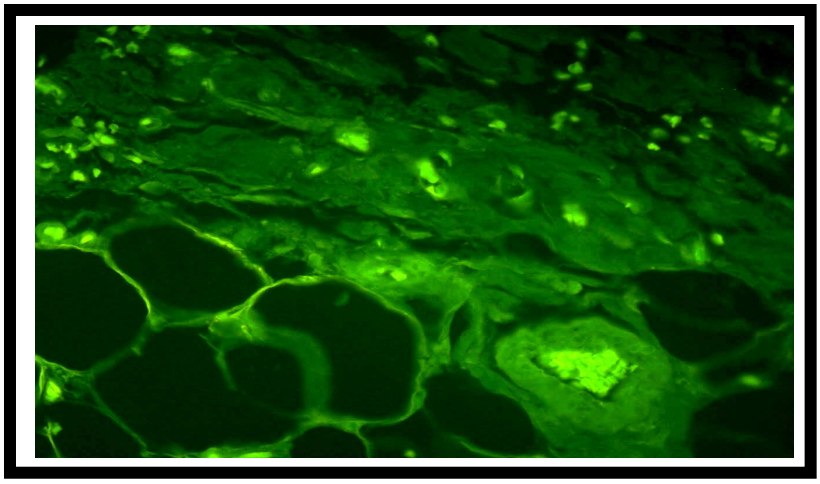

(B)

Figure 50: B-ACBP localization within fat cells of low and high-grade carcinoma
(A) Low grade dysplastic tissue sample illustrating a high level of localization within the fat cells of the 3’B-ACBP probe. (B) High grade dysplastic tissue sample shows an even higher level of localization within the fat cells and also in the adjacent tissue layer. Magnification X400.

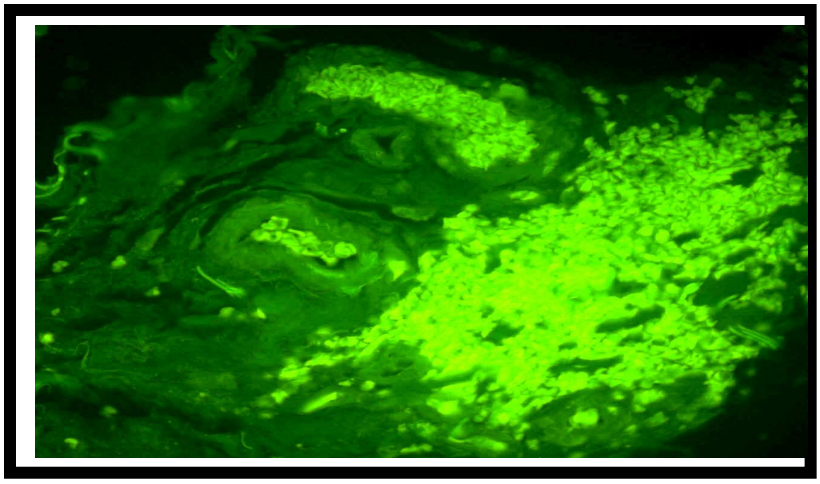

(A)

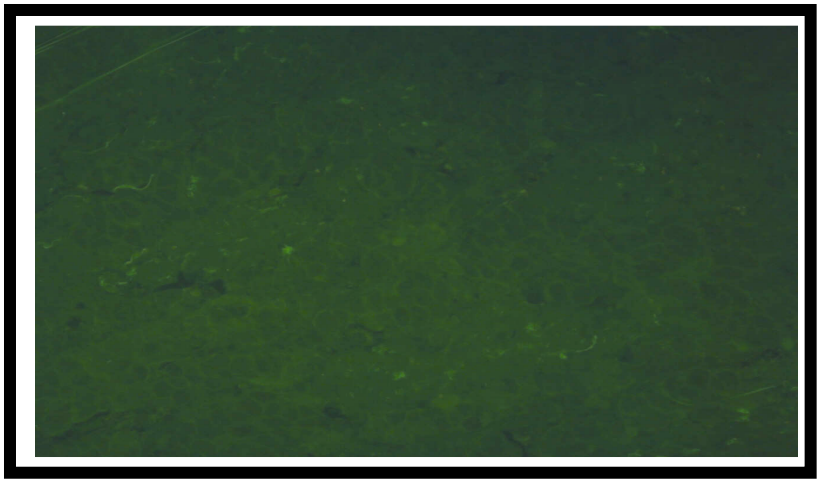

(B)

Figure 51: 3'B-ACBP FITC ISH results

(A) This is a muscularis mucosa section of a low grade dysplatic tissue sample and the 3'B-ACBP probe is localizing to the red blood cells produced by the blood vessels present. (B) Negative control of the muscularis mucosa section of the high grade tissue sample of the oesophagus. Magnification X400.

3.2.1.3.2.3 PBR Flourescent probes

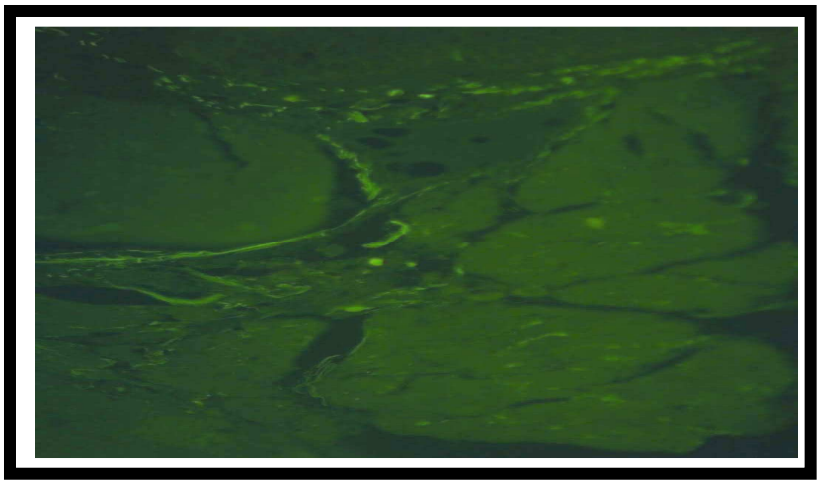

(A)

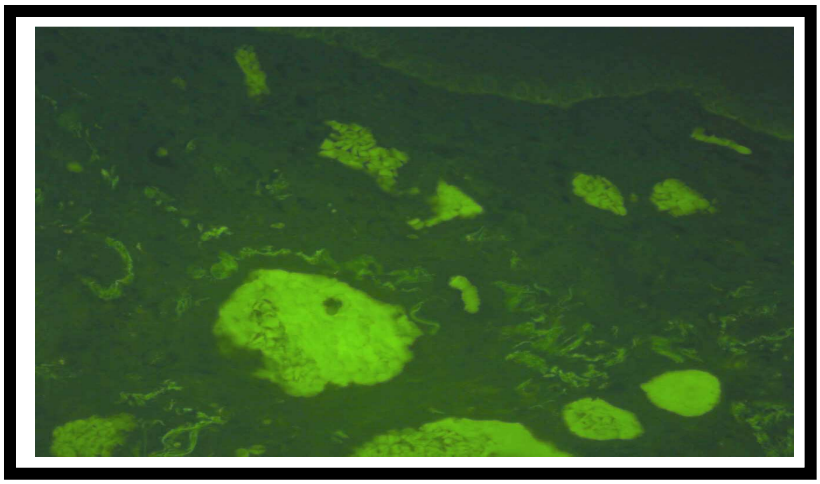

(B)

Figure 52: PBR localization in the mucosa of normal and diseased oesophagus

(A) This micrograph confirms the localization of PBR to the lamina propria is upregulated in a well-differentiated low grade squamous cell carcinoma, compared to (B) where no localization is seen in a normal oesophageal tissue section. Magnification X100.

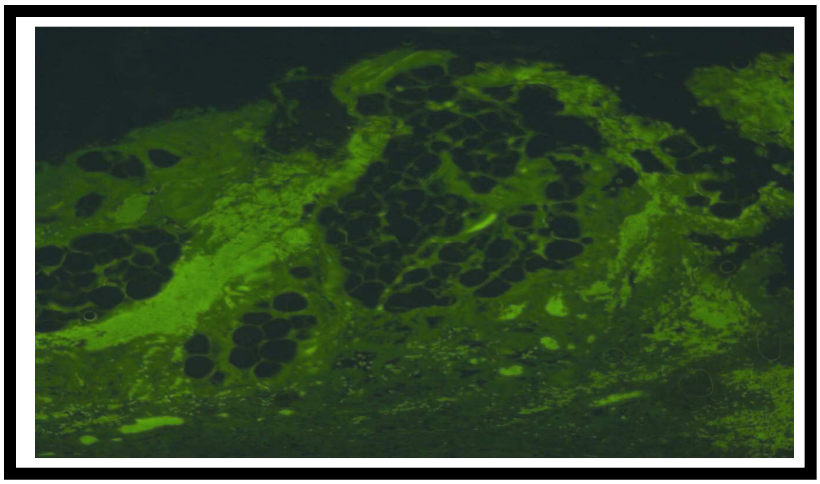

(A)

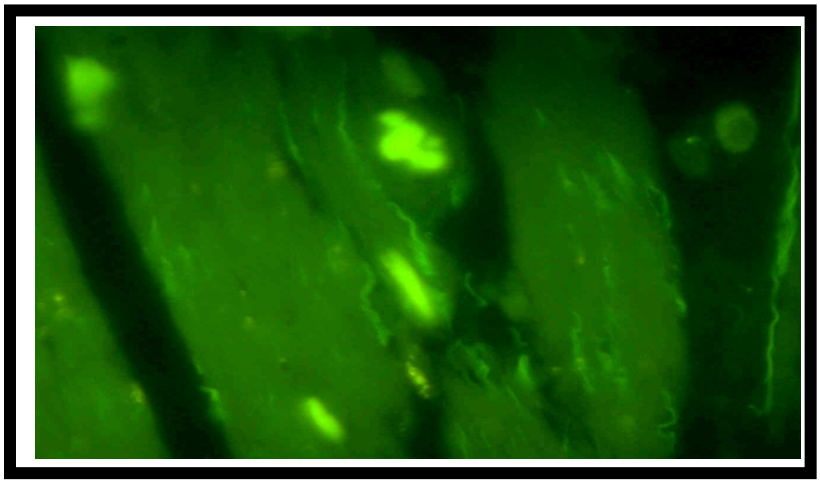

(B)

Figure 53: FITC ISH results of the PBR probe

(A) Fat cells of a low-grade dysplatic tissue sample show upregulation of the PBR probe. Magnification X100. (B) Localization of the PBR probe is seen in the fibroblast cells of the skeletal muscle of a high-grade invasive squamous cell carcinoma. Magnification X400.

Summary of expression and localization of 1-ACBP, B-ACBP and PBR in the differerent layers of the diseased and normal oesophagus.

Table 21: 1-ACBP expression and localization results

	Normal Oesophagus	Diseased Oesophagus
Epithelium	-	-
Lamina Propria	+	+++
Muscularis Mucosa	-	+++
Submucosa	-	+++
Circular muscle layer	-	+++
Connective tissue	+	+++
Longitudinal muscle layer	-	+++
Adventitia	-	-

Table 22: B-ACBP expression and localization results

	Normal Oesophagus	Diseased Oesophagus
Epithelium	-	+++
Lamina propria	-	+++
Muscularis Mucosa	++	+++
Submucosa	-	+++
Circular muscle layer	-	+
Connective tissue	+	+++
Longitudinal muscle layer	-	+
Adventitia	-	-

Table 23: PBR expression and localization results

	Normal Oesophagus	Diseased Oesophagus
Epithelium	-	-
Lamina propria	-	+++
Muscularis Mucosa	-	+
Submucosa	-	+++
Circular muscle layer	-	+
Connective tissue	+++	+++
Longitudinal muscle layer	-	+
Adventitia	-	-

- **No expression**
+ **Low expression**
++ **Moderate expression**
+++ **High expression**

3.2.1.4 Summary

All three genes showed substantial upregulation within the malignant tissue sections compared to normal oesophageal sections, within the lamina propria, muscularis mucosa, submucosa, connective tissue and longitudinal muscle layers. All five transcripts localized specifically and mainly to plasma cells and then lymphocytes in diseased and normal tissue section, with an increase in expression as the disease progressed and plasma cells increased. 3' and 5' Probes of 1-ACBP and B-ACBP was found to show similar results in degree and localization of expression, which was expected. The ACBP transcripts localized to endothelial cells in arteries within the connective tissue of diseased submucosa, but no localization was found in these cells in the normal oesophageal submucosa. B-ACBP localized to the nucleus in epithelial cells of the transformed epithelium, but no localization of this gene was found when compared to the normal epithelial cells. PBR was localized to tumour islands in invasive squamous carcinomas. Since all three genes are localizing to plasma cells and some lymphocytes, there is a possibility that these genes may be interacting with each other in some way to play a role in the immunological response to cancer cells. Quantitative RT-PCR illustrated PBR expression level was the highest compared to the ACBP genes expression in tumours, with the ACBP genes having comparative levels of transcripts.

3.3 The expression and purification of 1-ACBP, b-ACBP and PBR

3.3.1 Introduction

In situ hybridization studies showed an increase in expression of the three genes at the mRNA level in diseased tissue compared to normal tissue. Protein localization studies were intriguing as to determine whether the increase in the three proteins would be parallel to their mRNA expression. Further protein studies required the generation of antibodies, and therefore this study was carried out to express and purify the proteins for the generation of antibodies in rabbits, which would be useful for further immunohistochemistry analysis.

3.3.1.1Cloning of 1-ACBP, B-ACBP and PBR into pGEX-6P-2

3.3.1.1.1 RT-PCR amplification of 1-ACBP, B-ACBP and PBR ORF cDNA

PCR primers were designed based on the cDNA sequence of these genes obtained from the NCBI site; www.ncbi.nih.nlm.gov.Two sets of primers were designed for each gene, the first set designed to amplify the entire gene coding sequence to increase specificity, and the second set of primers were designed to contain restriction enzyme sites for the purpose of sub-cloning into the expression vector, pGEX6p2. The forward primers were designed to include a Bam HI restriction enzyme site and the reverse primers were designed to contain an Xho I restriction enzyme site as well as an additional stop codon. (Table 3.2.1) RNA was extracted from normal kidney cell lines and used as template for RT-PCR. The cDNA generated was used as template for PCR amplification, utilizing the specific primers designed the desired fragments containing restriction enzyme sites of 1-

ACBP (330 bp), B-ACBP (270 bp) and PBR (510bp) were generated (Figure 51 and Figure 52).

3.3.1.1.2 Cloning of 1-ACBP, b-ACBP and PBR gene sequences into pGEM-T-Easy.

The three PCR fragments containing restriction enzyme sites of 1-ACBP, b-ACBP and PBR were cloned into pGEM-T-Easy vector. Colony PCR was used to screen for positive colonies. Each amplification showed a positive result indicating that the desired PCR fragments were successfully cloned into the pGEM-T-Easy vectors. Small-scale plasmid isolation was prepared from a single clone for each gene utilizing the DNA miniprep kit from Promega.^{TM} Once the plasmid DNA from each clone was purified, a double digest was performed on the DNA purified using the restriction enzymes Xho I and Bam HI. Agarose gel electrophoresis was performed to determine whether the insert was released from the vector.

3.3.1.1.3 Sequencing

Sequencing analysis was performed at Inqaba bitotech, and M13 forward and reverse primers were used to determine whether the entire open reading frame plus restriction enzyme sites were present in the clones isolated and also whether any mutations occurred within the gene sequence. Sequence alignments between the human cDNA sequences of each gene (obtained from the NCBI site) and the insert sequence, and it showed a 100% identity between the compared sequences, confirming the result that the desired sequences have been cloned into the pGEM-T-Easy vector, with no mutations occurring within sequences.

3.3.1.1.4 Sub-Cloning 1-ACBP, b-ACBP and PBR gene sequences into pGEX-6P-2

The fragments released from the double digestion with XhoI and BamH I, were purified from agarose gels after electrophoresis using the DNA purification kit from Promega™. The purified fragments were thereafter cloned into the BamH I and Xho I site of the GST fusion vectors PGEX-6P-2 (Amersham Pharmacia®). Only two ORFs of the B-ACBP and PBR gene sequences were successfully subcloned. These plasmid DNA contsructs were transformed into competent *E.coli* BL21 Star™ pLys (DE3) cells.

3.3.1.1.5 Sequencing results:

B-ACBP and PBR pGEX clones were then sent to Inqaba biotech for sequencing. B-ACBP and PBR pGEX clone sequencing results are viewed in figures 53 and 54.

3.3.1.1.6 Expression and purification of B-ACBP and PBR

The pGEX clones were grown in LB containing ampicillin and induced with IPTG for a 16 hr period at 25 degrees Celcius.

3.3.1.1.7 Screening for the expression and solubility of B-ACBP

The transformed *E.coli* cells were screened for the expression of the recombinant GST proteins. Figure55 shows the total bacterial protein lysates for B-ACBP and PBR, induced by the addition of 0.1mM IPTG. The expected size of the recombinant GST-B-ACBP protein is approximately 37 kDa (GST=27kDa + B-ACBP=9.8kDa) and GST-PBR recombinant protein approximately 47kDa (GST=27kDa + PBR=20kDa), and as seen the expected protein size was not found.

Table 24: Primer sets of 1-ACBP, b-ACBP and PBR ORFs.

Gene	Primer sequences (set 1)	Primer sequences (set2)
1-ACBP	Fwd: ttgtctgagaccgagctatgtg	Fwd: ggatccatgggcgacctctg
	Rev: ggtttaacaggttattttcccg	Rev: cgctcgactcatatcccgtatt
b-ACBP	Fwd: gacaacagcagcagcaacaac	Fwd: attggatccatggccctgcag
	Rev: gcctctccctctaaatgttag	Rev: gcattgctcgagctaaattccg
PBR	Fwd: ctgaacagcagctgcagcag	Fwd: aattaggatccatggcccg
	Rev: catcacaagcgtgatggcac	Rev: gaactcgagtcactctggcag

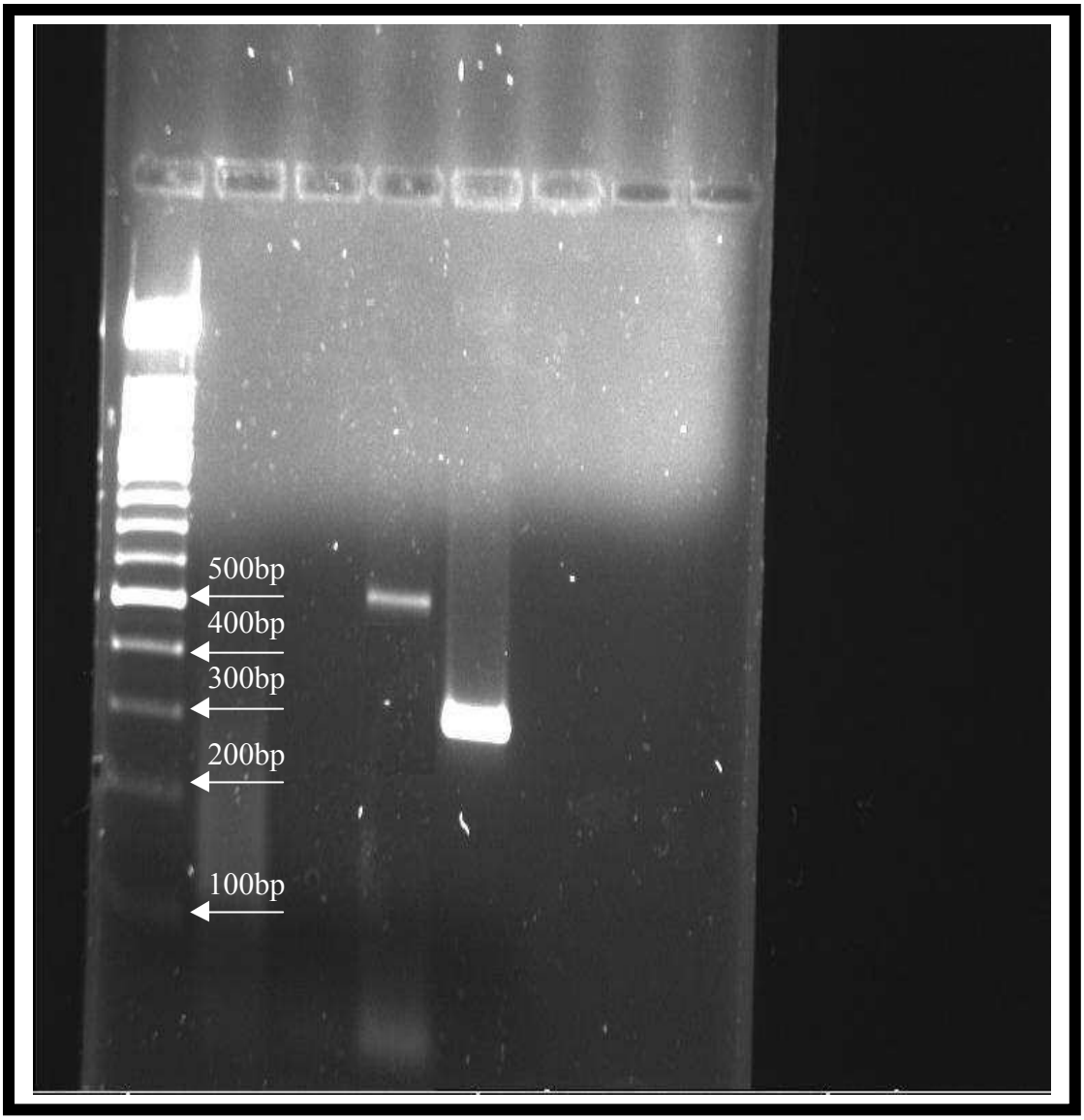

Figure 54: RT-PCR products of PBR and 1-ACBP ORF:

Lane 1: 100bp Molecular weight marker; Lane 4: RT-PCR product of the PBR open reading frame with restriction enzyme sites (ORF) with an expected base pair size of 510bp; Lane 5: RT-PCR product of 1-ACBP (ORF), with an expected base pair size of 330bp.

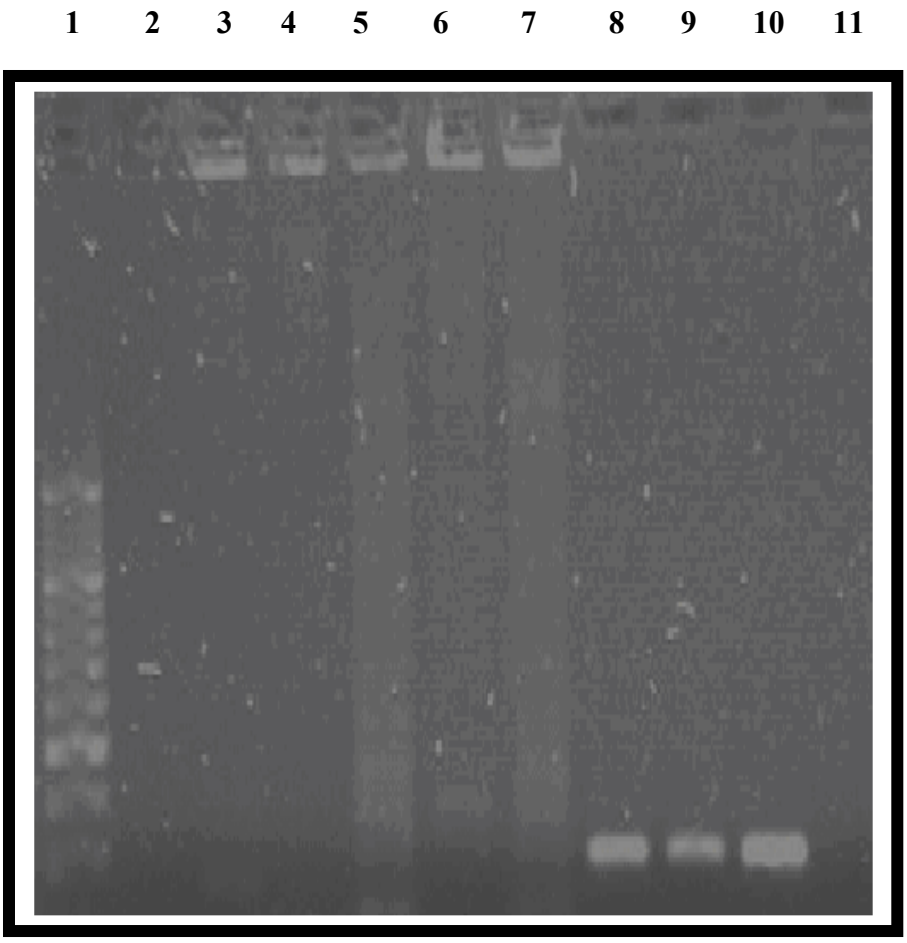

Figure 55: B-ACBP RT-PCR products

Lane 1: 100bp molecular weight marker; Lanes 8-10: Expected product size of B-ACBP ORF of approximately 270 bp. Lane 11: negative control (H_2O).

Figure 56: ORF sequence of B-ACBP in pGEX in the correct open reading frame

B-AC ORF

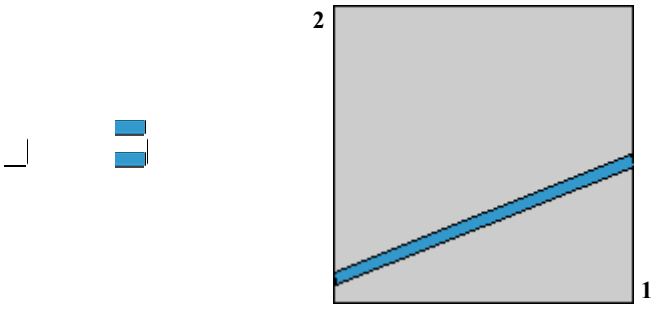

Identities = 265/267 (99%)



```
Query: 1   atggccctgcaggctgattttgacagggctgcagaagatgtgaggaagctgaaagcaaga 60
           ||||||||||||||||||||||||||||||||||||||||||||||||||||||||||||
Sbjct: 59  atggccctgcaggctgattttgacagggctgcagaagatgtgaggaagctgaaagcaaga 118

Query: 61  ccagatgatggagaactgaaagaactctatgggctttacaaacaagcaatagttggagac 120
           ||||| ||||||||||||||||||||||||||||||||||||||||||||||||||||||
Sbjct: 119 ccagaggatggagaactgaaagaactctatgggctttacaaacaagcaatagttggagac 178

Query: 121 attaatattgcgtgtccaggaatgctagatttgaaaggcaaagccaaatgggaagcatgg 180
           |||||||||||||||||||||||||||||| ||||||||||||||||||||||||||||
Sbjct: 179 attaatattgcgtgtccaggaatgctagatttaaaaggcaaagccaaatgggaagcatgg 238

Query: 181 aacctcaaaaaagggttgtcgacggaagatgcgacgagtgcctatatttctaaagcaaag 240
           ||||||||||||||||||||||||||||||||||||||||||||||||||||||||||||
Sbjct: 239 aacctcaaaaaagggttgtcgacggaagatgcgacgagtgcctatatttctaaagcaaag 298

Query: 241 gagctgatagaaaaatacggaatttag 267
           |||||||||||||||||||||||||
Sbjct: 299 gagctgatagaaaaatacggaatttag 325
```

atg: start codon
tag: stop codon

Figure 57: ORF sequence of PBR in pGEX in the correct open reading frame

PBR ORF

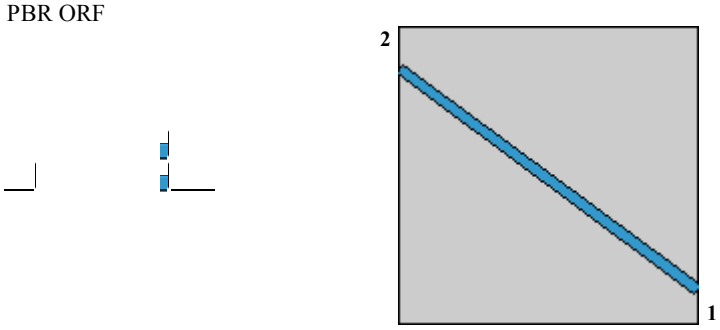

Identities = 510/510 (100%)



```
Query: 1   atggccccgccctgggtgcccgccatgggcttcacgctggcgcccagcctggggtgcttc 60
           ||||||||||||||||||||||||||||||||||||||||||||||||||||||||||||
Sbjct: 590 atggccccgccctgggtgcccgccatgggcttcacgctggcgcccagcctggggtgcttc 531


Query: 61  gtgggctcccgctttgtccacggcgagggtctccgctggtacgccggcctgcagaagccc 120
           ||||||||||||||||||||||||||||||||||||||||||||||||||||||||||||
Sbjct: 530 gtgggctcccgctttgtccacggcgagggtctccgctggtacgccggcctgcagaagccc 471


Query: 121 tcgtggcacccgccccactgggtgctgggccctgtctggggcacgctctactcagccatg 180
           ||||||||||||||||||||||||||||||||||||||||||||||||||||||||||||
Sbjct: 470 tcgtggcacccgccccactgggtgctgggccctgtctggggcacgctctactcagccatg 411


Query: 181 gggtacggctcctacctggtctggaaagagctgggaggcttcacagagaaggctgtggtt 240
           ||||||||||||||||||||||||||||||||||||||||||||||||||||||||||||
Sbjct: 410 gggtacggctcctacctggtctggaaagagctgggaggcttcacagagaaggctgtggtt 351


Query: 241 cccctgggcctctacactgggcagctggccctgaactgggcatggcccccccatcttcttt 300
           ||||||||||||||||||||||||||||||||||||||||||||||||||||||||||||
Sbjct: 350 cccctgggcctctacactgggcagctggccctgaactgggcatggcccccccatcttcttt 291


Query: 301 ggtgcccgacaaatgggctgggccttggtggatctcctgctggtcagtggggcggcggca 360
           ||||||||||||||||||||||||||||||||||||||||||||||||||||||||||||
Sbjct: 290 ggtgcccgacaaatgggctgggccttggtggatctcctgctggtcagtggggcggcggca 231


Query: 361 gccactaccgtggcctggtaccaggtgagcccgctggccgcccgcctgctctacccctac 420
           ||||||||||||||||||||||||||||||||||||||||||||||||||||||||||||
Sbjct: 230 gccactaccgtggcctggtaccaggtgagcccgctggccgcccgcctgctctacccctac 171


Query: 421 ctggcctggctggccttcgcgaccacactcaactactgcgtatggcgggacaaccatggc 480
           ||||||||||||||||||||||||||||||||||||||||||||||||||||||||||||
Sbjct: 170 ctggcctggctggccttcgcgaccacactcaactactgcgtatggcgggacaaccatggc 111


Query: 481 tggcatgggggacggcggctgccagagtga 510
           ||||||||||||||||||||||||||||||
Sbjct: 110 tggcatgggggacggcggctgccagagtga 81
```

atg: start codon
tga: stop codon

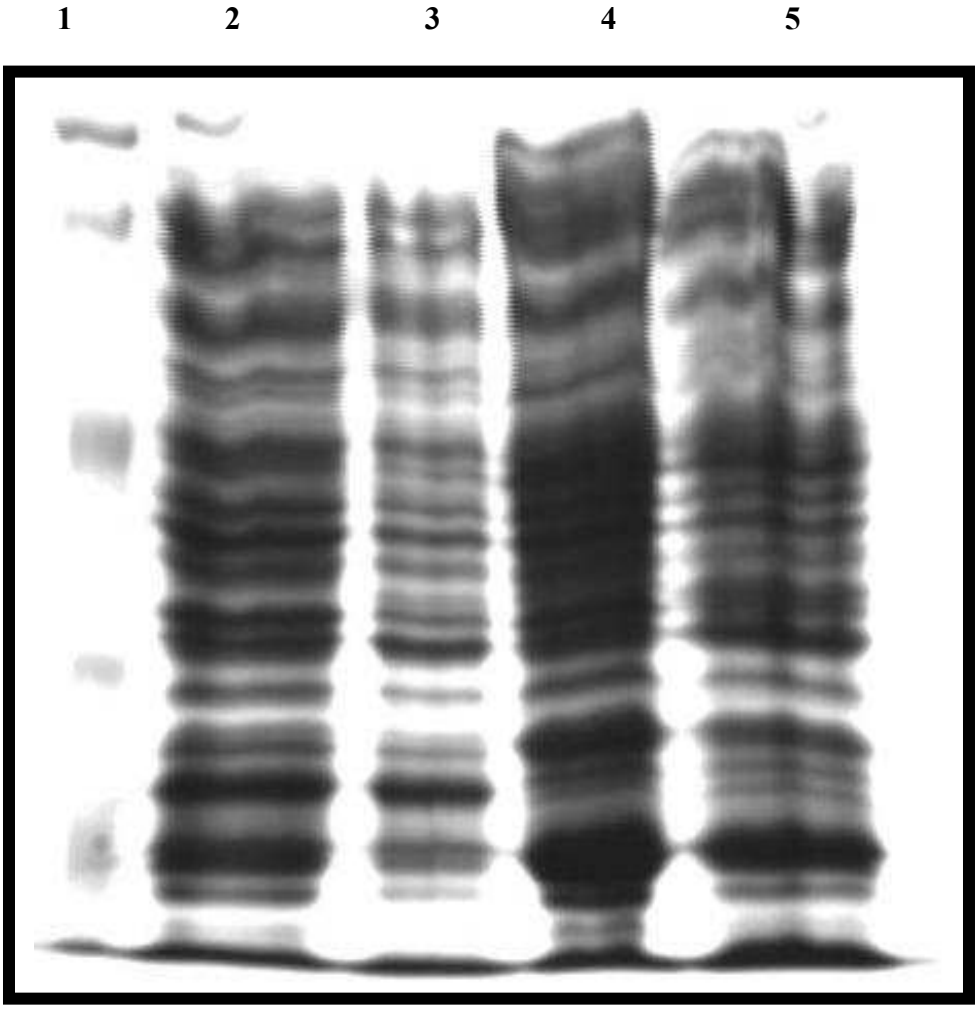

Figure 58: PBR and B-ACBP protein lysates on an SDS page gel

Lane 1: Protein molecular weight marker; Lane 2: PBR crude extract; Lane 3: PBR protein lysate from freeze-thaw cycles. Lane 4: B-ACBP crude extract; Lane 5: B-ACBP protein lysate from freeze thaw cycles.

3.3.2 Summary

PCR amplification of the genes of 1-ACBP, b-ACBP and PBR were accomplished via RT-PCR using RNA from a normal kidney cell line and two sets of primers. The desired fragments were subcloned into pGEM-T-Easy vectors, and the identity of these inserts were confirmed by colony PCR, restriction digestion and sequencing analysis. These inserts were then cloned into pGEX-6P-2. Only two ORF insert were successfully subcloned into pGEX, which was B-ACBP and PBR. B-ACBP and PBR expression was induced by the addition of IPTG. The proteins were lysed from the cells using the freeze-thaw method but an unexpected result was obtained.

3.4 Quantitative Gene analysis of 1-ACBP, B-ACBP and PBR in oesophageal cancer

Expression levels of 1-ACBP, B-ACBP and PBR were quantified in oesophageal cancer. RT-PCR was performed to obtain cDNA from disease oesophageal cancer. This cDNA was used as template and the sets of primers used were those designed for the probe sequences, and open reading frames of all three genes. The probe sequences of each gene was compared to its open reading frame gene product, to determine if the same expression level was obtained, and the three open reading frames of the three genes were also compared to each other to determine which concentrations were the highest.

The PCR products of the different genes were detected by measurement of SYBR Green 1 dye, which emits a fluorescence signal at wavelength 530nm when bound to double stranded DNA. The amplification curve is therefore created by an increase in SYBR Green 1 flourescence, which is directly proportional to the amount of double-stranded DNA generated as seen in figure 57 below.

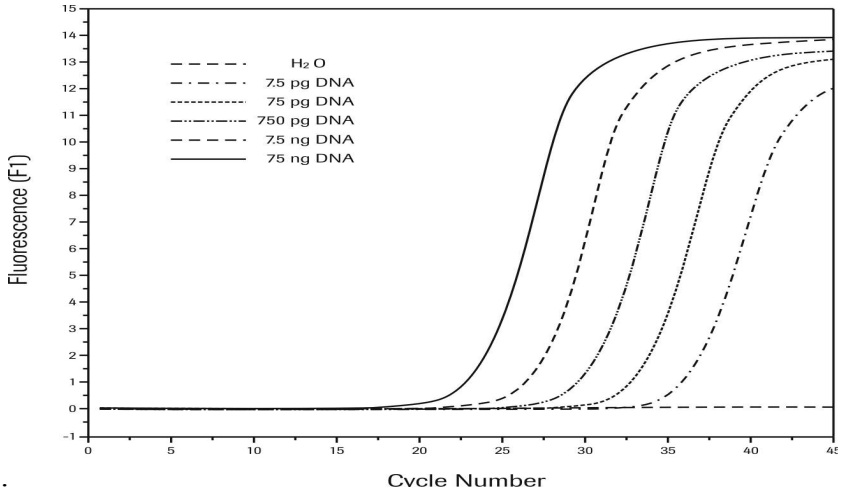

.

Figure 59: Amplification curves in the quantification module of the LightCycler Software 3.5 (channel F1, arithmetic baseline adjustment).

http://www.roche-applied-science.com/pack-insert/3515869a.pdf

3.4.1 Relative Quantification of 1-ACBP in oesophageal cDNA:

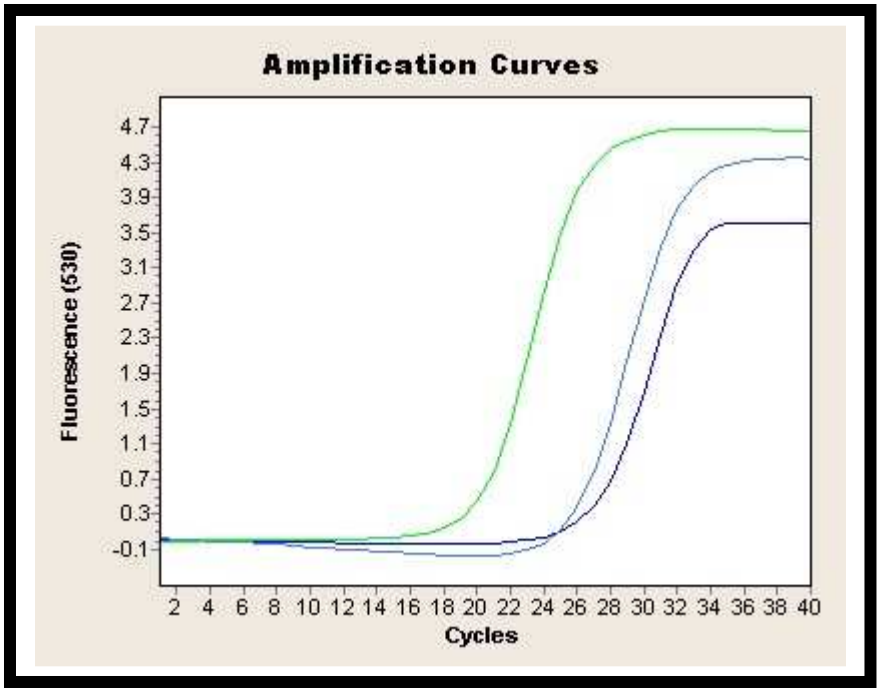

- 3' 1-ACBP
- 5' 1-ACBP
- ORF of 1-ACBP

Figure 60: 3'/ 5' and open reading frame expression correlation of the 1-ACBP gene
Comparison of 3' and 5'1-ACBP shows a higher concentration of 3'1-ACBP occurring in the oesophageal cancer cDNA than 5'1-ACBP. This could be due to primer annealing efficiency or even pipetting inefficiency. The open reading frame of 1-ACBP showed a comparable concentration with that of 5'1-ACBP, this is expected as these DNA products are from the same gene.

3.4.2 RelativeQuantification of B-ACBP in oesophageal cancer cDNA:

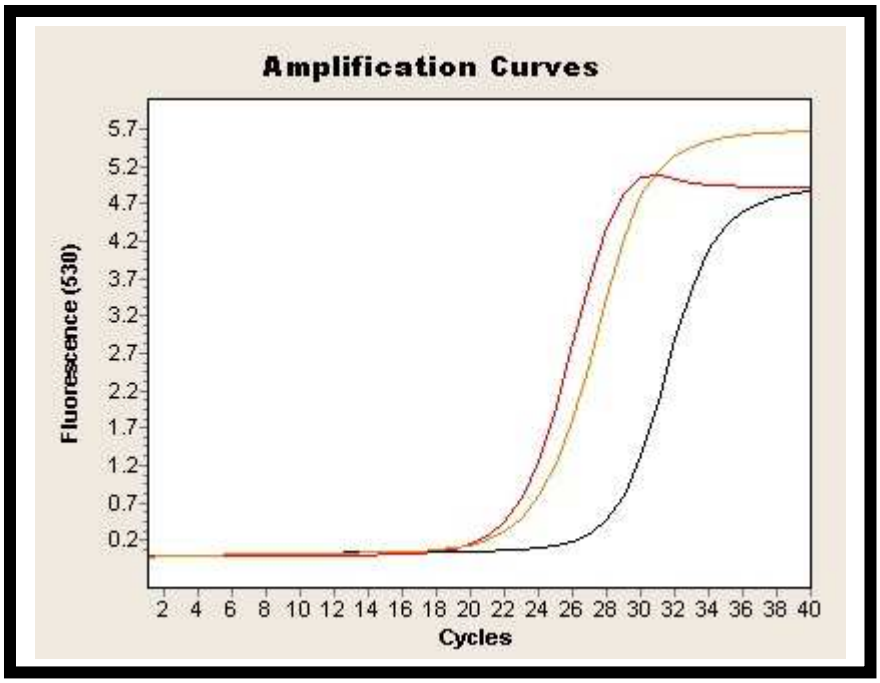

- **5' B-ACBP**
- **3' B-ACBP**
- **ORF of B-ACBP**

Figure 61: 3'/ 5' and open reading frame expression correlation of the B-ACBP gene

3' and 5' B-ACBP shows a comparable concentration level with each other, which is expected. The open reading frame of B-ACBP showed to be of a smaller concentration compared to the 3' and 5' sections of the gene. This again could be due to primer annealing efficiency or even pipetting inefficiency.

3.4.3 Relative Quantification of PBR in oesophageal cancer cDNA:

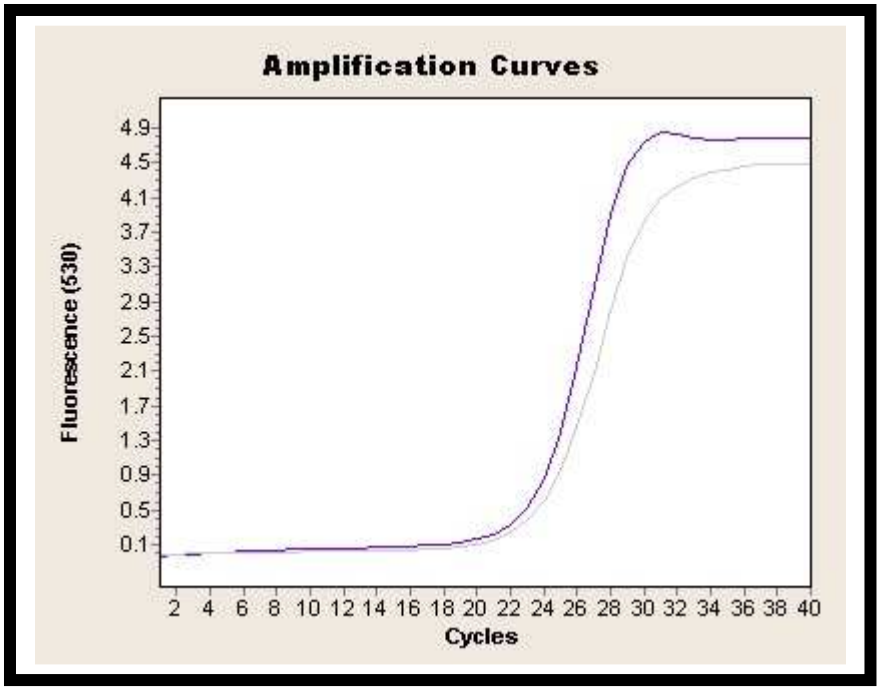

- **PBR probe cDNA**
- **ORF of PBR**

Figure 62: PBR probe cDNA sequence and the open reading frame expression correlation

The cDNA of the PBR probe sequence was compared with that of the entire open reading frame and a comparable concentration was found as expected.

3.4.4 Relative Quantification and correlation of 1-ACBP, B-ACBP and PBR in oesophageal cancer:

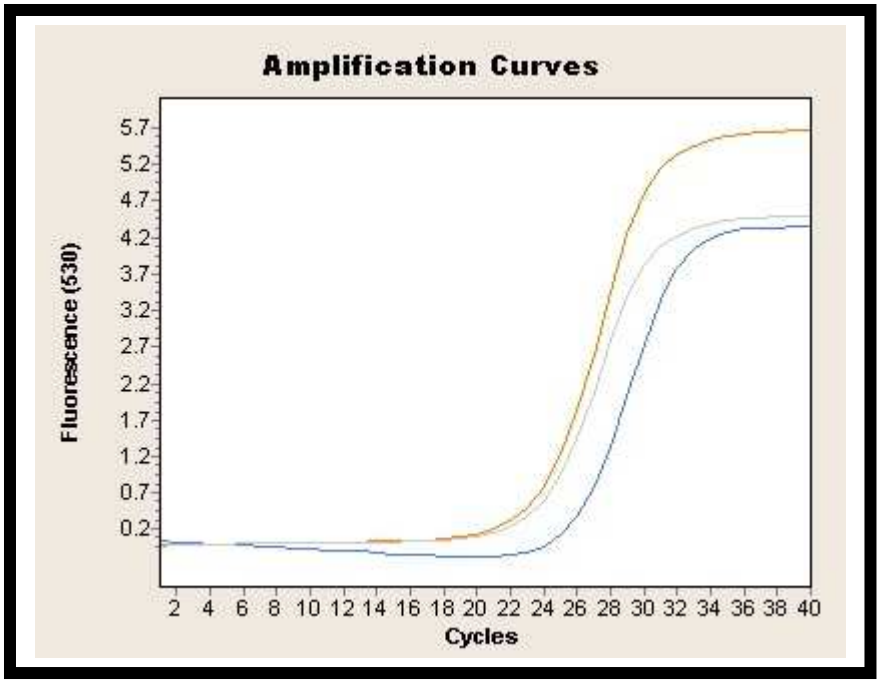

- **B-ACBP ORF**
- **PBR ORF**
- **1-ACBP ORF**

Figure 63: Open reading frame gene expression of 1-ACBP, B-ACBP and PBR

The three ORF expressions showed comparable expression results, with B-ACBP showing the highest level of expression, PBR second highest and 1-ACBP lower than the other two gene expression levels.

3.4.5 Summary

3’ and 5’ 1-ACBP cDNA fragments showed a considerable difference in amplification of PCR products obtained, which was not expected. However when 5’1-ACBP was compared to the open reading frame of 1-ACBP, it showed a comparable PCR product amplification, which means the same gene is being amplified. 3’1-ACBP primer annealing may therefore not be as efficient in binging therefore not generating as much product as the primers of 5’1-ACBP and the open reading frame of 1-ACBP.

3’ and 5’ B-ACBP amplification products concentration were similar to each other which was expected. Although when compared to the open reading frame of B-ACBP, it showed the open reading frame concentration was much lower compared to the 3’ and 5’ concentrations. This could be due to a higher concentration of B-ACBP mRNA transcript fragments that do not contain the entire open reading frame compared to the entire open reading frame concentration in the diseased cDNA.

PBR probe sequence that contains part of exon 1 and exon 2 compared to the open reading frame sequence of PBR generated comparable concentrations in the diseased cDNA as expected.

The open reading frames of 1-ACBP, B-ACBP and PBR concentrations were compared and showed comparable expression levels, with B-ACBP having the highest concentration, PBR second highest and 1-ACBP the lowest.

.